M-PM-Sym-1

STRUCTURAL BIOLOGY OF HOMOPHILIC CELL ADHESION.
(Wayne A. Hendrickson*‡, Lawrence Shapiro*, Peter D. Kwong*, Allison M. Fannon#, Joseph P. Doyle#, and David R. Colman#) Department of Biochemistry and Molecular Biophysics* and Howard Hughes Medical Institute‡, Columbia University, New York, NY 10032; and Brookdale Center for Molecular Biology#, Mt. Sinai School of Medicine, New York, NY 10029.

In many instances the organization of cells into tissues involves interactions between like molecules from the contacting cell surfaces. Homophilic adhesion can also be important between membrane surfaces of the same cell as in the myelin sheath covering nerve axons. The molecules that subserve these extracellular interactions traverse the membrane, and cytoplasmic portions may mediate other interactions, which in the case of cadherins are to cytoskeletal elements such as actin filaments. We have determined the structure of an adhesive domain of N-cadherin in three crystal lattices, all of which exhibit a common interdigitated ribbon of these domains. The features of this ribbon are like those expected for the natural cell-cell interface, which we describe as a cell adhesion zipper. We have also determined the crystal structure of the P0 adhesion domain from peripheral nerve myelin. In this crystal as well, features of the packing appear to relate to the natural adhesive interaction. Cooperative superstructures such as these may in general provide a mechanism to marshal individually weak molecular interactions into strong bonds between cells.

M-PM-Sym-2

STRUCTURE AND FUNCTION OF A HETEROTRIMERIC G-PROTEIN.
((H. Hamm)) University of Illinois at Chicago.

M-PM-Sym-3

STRUCTURAL BASIS FOR SPECIFICITY IN PROTEIN-TYROSINE KINASE SIGNALING.
((Lewis Cantley and Zhou Songyang)) Division of Signal Transduction, Beth Israel Hospital and Dept. of Cell Biology, Harvard Medical School, Boston, MA 02115

Protein kinases find their downstream targets by a series of selection procedures based on the structure of the kinase and its target. To address the specificity of domains involved in protein kinase/substrate interactions we developed a novel "oriented peptide library" technique. Using a phosphotyrosine peptide library we were able to determine the optimal. peptides for binding to most of the known src-homology 2 (SH2) domains These studies have led to the conclusion that residues immediately C-terminal of the phosphoTyr moiety are critical for determining specificity in binding. In contrast, this same approach showed that the recently-described PTB/PID domains have specificity for phosphoTyr peptides based on residues N-terminal of the phosphoTyr motif. We also developed a library of oriented peptide substrates for kinases and were able to determine the optimal nonapeptide substrate for 9 different protein-tyrosine kinases. We found that the sequences of the optimal substrates of individual protein-tyrosine kinases matched the optimal sequences for binding to subgroups of SH2 domains suggesting that the protein-tyrosine kinases pre-select sights that will recruit subgroups of SH2-containing proteins. By modeling the optimal peptides into known structures of these domains it has been possible to predict which residues on the proteins are involved in specific recognition. Mutational studies have provided tests of these predictions. This approach also allows one to make predictions about targets of protein kinases on the basis of linear sequences .

M-PM-Sym-4

STRUCTURE AND MECHANISM IN CELLULAR SIGNAL TRANSDUCTION
(S.C. Harrison) HHMI/Harvard, Cambridge, MA 02138

The talk will review our understanding of the structural mechanism of specific recognition of phosphotyrosyl peptides by SH2 domains, as illustrated by work from the author's laboratory and from other groups.

K CHANNEL GATING I

M-PM-A1

EARLY EVENTS IN VOLTAGE GATING
((E. Stefani and F. Bezanilla)) Departments of Anesthesiology and Physiology, UCLA, Los Angeles, CA 90095-1778

Gating currents of *Shaker B* K^+ channels show a rising phase upon depolarizations that exceed -40 mV when recorded with bandwidths below 10 kHz. With extended bandwidths, the rising phase is preceded by a fast transient peak component. To observe this component, the patch clamp amplifier has been modified to extend its bandwidth beyond 200 kHz and the acquisition system has been upgraded to sample at 5 MHz. The capacity transient of large macro patches in oocytes decays with a time constant of less than 2 µs. Under these conditions, gating currents show a large early component that rises as fast as the settling time of the capacity transient and decays with a time constant of about 8 µs at 0 mV at room temperature. The peak value of this initial component may be up to 3 times as large as the peak of the on gating current and it is critically dependent on the speed of the voltage clamp. Its amplitude can be dramatically reduced in cases when the capacity transients have a slower component, most likely produced by membrane that has been invaginated too deeply in the pipette and is charged by a larger series resistance. The charge carried by the initial component is proportional to the amount of the total charge in the same patch indicating that they are related and the charge transported by the peak is less than 10% of the gating charge. The voltage dependence of the charge transported by this component is shallow (z<1) and tends to saturate near +50 mV, but we did not detect a clear saturation at the negative potentials explored (*ca.* -200 mV). The peak value of this initial component decreases with a slower decay as the temperature is lowered. The initial component is not dependent on the presence of permeant or impermeant ions; also, it does not depend on the presence of divalent ions nor changes when pH is made more alkaline (pH=8). These results indicate that this charge movement is unlikely to be related to ion movement in the pore or vestibule of the channel. Instead, we believe that this fast component corresponds to early dipole rearrangements of the channel protein (such as alpha-helix tilting) preceding the large charge movement that gates the channel open. Supported by NIH GM 30376 and GM 52203 grants.

M-PM-A2

ENTROPIC AND ENTHALPIC CHANGES DURING *SHAKER* K+ CHANNEL ACTIVATION.
((B.M. Rodriguez*, D. Sigg, and F. Bezanilla)) IVIC*, POB. 21827. Caracas 1020A, Venezuela and Departments of Physiology and Anesthesiology, UCLA, Los Angeles, CA 90024.

We have extended the characterization of the temperature dependence (3-22° C) of ionic and gating currents (I_g) recorded from Shaker H4 K+ channels expressed in *Xenopus* oocytes (Rodriguez et. al., Biophys. Society, 1995). In order to study the temperature dependence of transitions close to the conducting state, we recorded ionic tail currents (I_{tail}) evaluated at -120 to -20 mV, following a maximally activating test pulse. Of the two principal exponentially decaying components of I_{tail}, the fast (τ = .3 to 1 ms, *ca.* 19° C) predominates at very negative potentials and mixes with the slow (τ = 3 to 30 ms, *ca.* 19° C) at more depolarized potentials. The Arrhenius plot is linear for both components (Q_{10} > 4). Kinetic components of I_g at depolarized potentials also have Q_{10}> 4, suggesting that the free energy transition barriers near the open state have a large enthalpic component. In contrast, the Cole-Moore shift in ionic current and the component of the gating current in the range -150 to -50 mV are both relatively temperature insensitive (Q_{10} <1.2), indicating that the earlier activation barriers have smaller enthalpic components. The conductance *vs.* voltage (G-V) at positive potemtials shows a shift to more depolarized potentials with lower temperature, in contrast to the gating charge *vs.* voltage (Q-V) curve, which is relatively temperature insensitive at depolarized potentials. Thus, it appears that lower temperatures de stabilize the open state relative to adjacent states. Non-stationary noise analysis of I_g in the range -10 to 40 mV shows no change in the elementary charge movement with temperature, supporting the notion that the magnitude of the individual charge movements are not affected by temperature. These data support our earlier hypothesis that the activation pathway for *Shaker* consists of multiple early transitions with small enthalpic contributions and a net negative entropic changes, followed by at least one transition with a large enthalpic change and a net positive entropic change.
Supported by USPHS grant GM30376 and BID-CONICIT and IVIC fellowships (Venezuela).

M-PM-A3

IDENTIFICATION OF A FIRST-ORDER GATING PROCESS IN SHAKER B CHANNELS((M.Rayner, M.Andres, H.Bao, M.Henteleff, M.Hermosura, J.Lu, and J.Starkus)) Békésy Lab, Pac. Biomed. Res. Ctr., Univ. Hawaii, Honolulu, HI 96822

The solvent-insensitivity seen in the time constants of both fast deactivation and fast reactivation (after very brief interpulse intervals) suggests that these processes may reflect a single, kinetically isolatable, first-order gating reaction. We present evidence from thermodynamic analysis of reaction kinetics which further supports this conlusion in inactivation-removed *Shaker* B channels. Using this analytic approach in a series of S4 charge-neutralization mutants provides evidence suggesting that no more than the 5th and 6th charges can cross the steep component of the membrane field in this isolated reaction step. This implies that the steep field region must be considerably compressed (in the zone of S4 movement), and probably no wider than the selectivity filter. However, if this conclusion is correct, then the steep field fraction can be no greater than ~50% of applied transmembrane potential. Therefore, a second step in S4 movement must be presumed (which, during monomer activation, would precede the step evaluated here). This additional step should involve movement of a further 2 (or 3) charges across the steep part of the field.

(Supported by PHS grant #NS-21151, and NIH RCMI grant #RR-03061)

M-PM-A4

QUASI-EQUILIBRIUM NOISE ANALYSIS OF *SHAKER* K^+ CHANNEL GATING CURRENTS. ((D. Sigg, E. Stefani, H. Qian, F. Bezanilla)) Departments of Physiology, Anesthesiology, and Biomathematics, UCLA, Los Angeles, CA, 90024.

What do fluctuations in the gating current (I_g) of a K^+ channel tell us about the movement of the voltage sensor? Until recently, we have measured only the non-stationary component of the I_g variance which follows a step pulse in voltage. Assuming a standard Markov jump process interpretation of the gating kinetics, non-stationary noise analysis tells us there is a major charge transition (q_{max}) which moves *ca.* 2.3 e_o. We have found the value of q_{max} to be robust, conserved over a range of depolarizing potentials, bandwidths, and temperatures. Despite the success of the jump process model, we find that, in a purely phenomenological way, we can also interpret our data as the "center of mass" coordinate (q) of the voltage sensor undergoing over damped Brownian motion (diffusion). The physical implications of these two interpretations are very different. Fluctuations in q for simple cases of diffusion may be unrelated to its directed motion. In contrast, for a jump process, the average motion of q and its fluctuations are intimately related - thus the variance of q and I_g (=dq/dt) will decrease at saturating regions of the equilibrium charge vs. voltage (Q-V) curve. To test this, we applied a slow (>50 msec) ramp potential which moved the voltage sensor of the *Shaker* H4ir W434F K^+ channel along its entire range, thereby tracing out a (quasi) Q-V curve in patches containing ~ 10^5 channels. I_g fluctuations in units of pF^2 vs. voltage were obtained from an ensemble of ramps (see figure). The magnitude and voltage dependency of the variance of I_g are generally consistent with that predicted by ramp simulations of jump processes. The size of the equilibrium fluctuations may prove difficult to reconcile with a diffusion process.

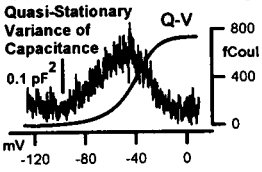

Supported by NIH GM30376.

M-PM-A5

IDENTIFICATION OF VOLTAGE SENSING RESIDUES IN SHAKER K^+ CHANNELS. ((S.-A. Seoh, D. Sigg, D.M. Papazian, and F. Bezanilla)) Department of Physiology UCLA School of Medicine, Los Angeles, CA 90095-1751

Basic residues in S4 and acidic residues in S2 and S3 segments of Shaker K^+ channels have been postulated to be responsible for charge movement of the voltage sensor but direct evidence has not been provided. We addressed this question by measuring the total gating charge per channel in mutants where each of these charged residues have been neutralized one at a time. One method was to estimate the number of channels (N) in the patch by fluctuation analysis and measure the gating current in the same patch to measure the total charge (Q) to compute Q/N. The second method was a measurement of the limiting slope at very negative potentials which gives an estimate of the charges directly coupled to opening. The inactivation-removed Shaker (IR) gave 13e per channel with both methods. We tested 2 acidics in S2 segment (E283 and E293), one acidic in S3 (D316) and 4 basic residues in S4 (R365, R368, R371, and K374). Q/N was decreased to 6-8e in E293Q, R368N, and R371Q. Neutralizations E283Q, D316N, and R365Q, and charge conserving mutations E293D and R368K showed normal Q/N. S4 position K374 was studied in two double mutants to rescue expression (Papazian et al., Neuron 14, 1995). Q/N in double mutants K374Q+D316N and K374Q+E293Q is the same as in the acidic neutralization alone, indicating that K374 does not contribute to the gating charge. Limiting slope measurements agreed with the Q/N measurements except for D316N and E283Q. These results show that E293, R368, and R371 contribute to the gating charge of the channel, and the large reduction in Q/N indicates that these single neutralization mutants have indirect effects on the movement of unmutated residues through the field. Supported by NIH grant GM30376 (FB,DS,SS) and Pew Charitable Trust (DMP).

M-PM-A6

EXTERNAL BARIUM INFLUENCES THE GATING CONFORMATIONAL CHANGES OF THE NON-CONDUCTING AND NON-INACTIVATING *SHAKER* K^+ CHANNEL, *Sh*H4-IR W434F. ((R. S. Hurst, M. J. Roux, L. Toro and E. Stefani)) UCLA, Dept. of Anesthesiology, Los Angeles, CA 90095-1778

In addition to occluding the conduction pathway, it has been proposed that Ba^{2+} inhibits K^+ channels by stabilizing the closed state (Armstrong and Taylor, 1980). If Ba^{2+} binding alters the voltage-dependent gating conformational changes, these changes should be evident in the gating current. We have previously reported that external Ba^{2+} does not modify the gating current of *Sh*H4-IR at potentials hyperpolarized to channel opening. However, in those studies the gating current could not be assayed at more depolarized potentials due to the evoked ionic current which obscures the former. Therefore, we tested the effects of external Ba^{2+} on the gating currents of the non-conducting mutant *Sh*H4-IR W434F expressed in *Xenopus* oocytes. In the absence of Ba^{2+}, the *off* gating current (Q_{off}), evoked upon repolarization, is normally slowed following depolarizing commands more positive than about -45 mV. This slow down is thought to reflect a rate limiting conformational change as the channel goes from the "open" to the first closed state (Perozo et al., 1993). Concentrations of Ba^{2+} up to 2 mM had no observable effect either on the kinetics or quantity of *on* gating current (Q_{on}). Q_{off} was not affected following depolarizations negative to -45 mV. However, for more positive depolarizations, populating the final states near the open conformation, external Ba^{2+} markedly increased the rate of gating charge return. This increased rate of Q_{off} can be accounted for by a scheme in which Ba^{2+} hinders the channel from reaching the final open state.

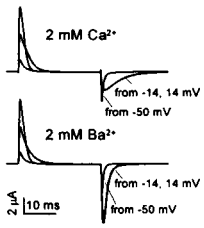

(Supported by NIH grant GM50550)

M-PM-A7

ROLE OF TRANSMEMBRANE SEGMENT S5 IN VOLTAGE-DEPENDENT GATING OF TWO CLONED VOLTAGE-GATED POTASSIUM CHANNELS. **(C.C. Shieh[1,2], K.J. Greene[2] and G.E. Kirsch[1,2]) Rammelkamp Center for Research[1], MetroHealth Medical Center and Department of Physiology and Biophysics[2], Case Western Reserve University, Cleveland, OH 44109.**

Kv2.1 and Kv3.1 are cloned voltage-gated K^+ channels with markedly different gating kinetics and sensitivity to the gating dependent blocker, 4-aminopyridine (4-AP). To uncover the structural determinant we measured gating currents in the two parent channels and a chimeric channel expressed in *Xenopus* oocytes using macropatch voltage-clamp technique. The charge versus potential (Q-V) curve revealed that the half-activation potential and the effective valence for Kv3.1 were 12.1 mV and 2.2 while -22 mV and 1.7 for Kv2.1, respectively. The kinetic analysis of gating currents showed two exponential components of gating current decay in both Kv3.1 and Kv2.1. Although the ON gating current decays slightly faster in Kv3.1 than that in Kv2.1, the OFF gating current in Kv2.1 is much slower than that in Kv3.1, consistent with the observation of slow deactivation of macroscopic ionic current in Kv2.1 compared to Kv3.1. In Kv3.1, 4-AP (0.1 mM) blocked slow component of gating current with ~10% reduction in total gating charge movement. A chimeric channel (5'S5), in which the cytoplasmic half of S5 in Kv2.1 was replaced with equivalent region of Kv3.1, renders the channel more sensitive to 4-AP blockade and has half-activation potential (-21 mV) and effective valence (1.7) similar to Kv2.1 but has OFF gating current kinetics similar to Kv3.1. Our results suggest that the cytoplasmic end of S5 may be an important structural determinant of the final activation steps that open the channel. (Supported by NIH grant 29473).

M-PM-A8

INVOLVEMENT OF S6 IN VOLTAGE-DEPENDENT DEACTIVATION GATING OF hKv1.5 POTASSIUM CHANNELS. ((D.J. Snyders, T.C. Rich, D.J. Mays, M.M. Tamkun and S.W. Yeola)) Vanderbilt University, Nashville, TN 37232.

Several residues in the S6 segment of voltage-gated K-channels have been proposed to line the ion conducting pore and to be molecular determinants for open channel block by quaternary ammonium (QA) derivatives. Analyzing the effects of several hKv1.5 mutations in S6 we observed significant effects on channel gating. The activation kinetics for mutations T505I, T505S, L508M, V512A, V512M and S515E were similar to WT when adjusted for shifts in the voltage-dependence of activation from WT (E_h= -15 mV) which were -6, +5, +11, -26, -31 and -10 mV, respectively. Deactivation kinetics between -40 and -140 mV for T505S were similar to WT. However, deactivation was significantly slowed with τ of 2.1, 7.2, 11, 78, 196 and 315 ms (at -110 mV) for WT, L508M, S515E, T505I, V512A and V512M, respectively. The degree of deactivation slowing was not related to the voltage shifts of activation; e.g. T505I altered primarily channel deactivation. The voltage-shift for S515E is opposite to that expected from a local charge effect on the voltage sensor. The slowing of channel deactivation for V512A and V512M corresponds to stabilization of open state by about 12 kJ/mole. Taken together, the results suggest that rate-limiting steps in channel activation and deactivation are controlled by conformational changes involving different structures, with S6 being involved in rate-limiting closing transitions. A possible interpretation of the results is that these residues are partially buried in the rested state and become exposed during channel activation. The effect of the mutations would be to slow proper refolding into the rested conformation. Supported by HL 47599.

M-PM-A9

RELATIONSHIP BETWEEN 4AP BINDING AND CHANNEL GATING IN Kv4.2 AND Kv1.4. ((G.-N. Tseng, B. Zhu, and J.-A. Yao)) Dept of Pharmacology, Columbia Univ., New York, NY 10032

4AP can block many native K channels with seemingly different state-dependences. The mechanism and channel structural determinants underlie the state-dependence of 4AP actions is not clear. We compared the kinetics of 4AP binding and unbinding in Kv4.2 and Kv1.4 expressed in Xenopus oocytes. 4AP was a "rested-state" blocker of Kv4.2 with an IC_{50} of 5-10 mM. Elevating $[K]_o$ slowed the rate of 4AP binding. In contrast, 4AP was an "activated-state" blocker of Kv1.4 with an IC_{50} of 0.4-1.2 mM. However, Kv4.2 and Kv1.4 shared the following similarities in 4AP actions: (1) 4AP blocked both from inside the cell, (2) For both, 4AP unbinding occurred in the open state and was enhanced by stronger depolarizations in the voltage range from -40 to +60 mV, (3) 4AP binding and the closure of the inactivation gate were mutually exclusive. Transferring the cytoplasmic half of the S5 transmembrane domain from Kv4.2 to Kv1.4 transferred the 4AP binding and unbinding characteristics. 4AP blocked this mutant channel of Kv1.4 in the rested-state and unblocked in the open-state with an IC_{50} of 5-10 mM, although the blocking and unblocking rates were 10 fold and 3-5 fold slower than those on Kv4.2, respectively. Based on these data, we propose the following: (1) The difference in the state-dependence of 4AP actions between Kv1.4 and Kv4.2 is only apparent, (2) 4AP binds within the channel pore, with the binding site protected by the activation and inactivation gates and the binding site affinity modulated by conformational changes involved in channel opening, (3) The "looseness" of the activation gate in preventing 4AP from gaining access to its binding site in the pore is different between Kv1.4 (tight) and Kv4.2 (loose), (4) The link between conformational changes during channel opening and 4AP unbinding differs between Kv1.4 (loose) and Kv4.2 (tight), (5) The cytoplasmic half of S5 is involved in the regulation of 4AP binding and unbinding by channel gating.

M-PM-A10

PROBING THE PORE OF AN INWARD-RECTIFIER K^+ CHANNEL WITH A SCORPION TOXIN. ((Zhe Lu, John H. Lewis and Roderick MacKinnon)) Department of Neurobiology, Harvard Medical School, Boston, MA 02115.

Lq2 is a charybdotoxin isoform known to block both Ca^{2+}- and voltage-activated K^+ channels. Scorpion toxins inhibit K^+ channels by binding to the external vestibule and occluding the ion conduction pore. It has been established in voltage-activated K^+ channels that the toxin binding site is largely contained within the P-region. We find that Lq2 blocks an inward-rectifier K^+ channel, ROMK1, with a K_i of 0.4 μM. Mutagenesis studies show that Lq2 inhibits ROMK1 by interacting with residues in the P-region. Many amino acids in the P-region that are important for toxin binding are not conserved among voltage-activated, Ca^{2+}-activated and inward-rectifier K^+ channels. This argues that the shape of the vestibule is similar in these three types of K^+ channels. The signature sequence (TXXTXGYG) within the P-region is a critical determinant of K^+ selectivity and is conserved among the three types of K^+ channels. This raises the intriguing possibility that Lq2 actually recognizes the signature sequence.

M-PM-A11

PROBING VOLTAGE-GATED K^+ CHANNELS WITH A NEW PEPTIDE INHIBITOR ((Kenton J. Swartz and Roderick MacKinnon)) Dept. of Neurobiology, Harvard Medical School, Boston, MA 02115.

We recently isolated a new peptide inhibitor of voltage-gated K^+ channels from spider venom. This inhibitor, which we named hanatoxin, inhibits the Kv2.1 and Kv4.2 K^+ channels with high affinity (K_d~40 nM). The Shaker K^+ channel and a number of its mammalian homologs are relatively insensitive to hanatoxin. Kv1.1, Kv1.3 and Kv1.6 are not inhibited by 500 nM hanatoxin, while the Shaker K^+ channel is only weakly inhibited (K_d~10 μM). Kv3.1, a Shaw-related K^+ channel and the eag K^+ channel are insensitive to 500 nM hanatoxin. The S5-S6 linker forms the binding site for a number of pore-blocking K^+ channel inhibitors such as charybdotoxin, agitoxin and dendrotoxin. To test whether the same region is important for inhibition by hanatoxin we constructed a number of chimeras by swapping regions of the Kv2.1 K^+ channel (hanatoxin sensitive) into the Shaker K^+ channel (hanatoxin insensitive). The Kv2.1 K^+ channel is insensitive to pore-blocking inhibitors, such as agitoxin, whereas the Shaker K^+ channel is very sensitive to agitoxin. When the S5-S6 linker from Kv2.1 is transferred to the Shaker channel agitoxin sensitivity is lost, consistent with previous results. However, hanatoxin sensitivity is not acquired and furthermore, the weak inhibition of the Shaker channel by hanatoxin is unaffected by the mutation. These results imply that hanatoxin interacts with a region of K^+ channels outside the S5-S6 linker. Transfer of the S1-S2 linker, S2-S3, or S6 from the Kv2.1 K^+ channel into the Shaker K^+ channel are without effect on hanatoxin sensitivity. In contrast, transfer of the S3-S4 linker from the Kv2.1 K^+ channel into the Shaker K^+ channel substantially increases hanatoxin affinity (K_d~400 nM). These results suggest that hanatoxin interacts with regions of voltage-gated K^+ channels that are distinct from those recognized by the pore-blocking peptides and that it should be a useful probe for studying the structure and function of these regions.

Ca CHANNELS AND E-C COUPLING

M-PM-B1

MODAL TRANSITIONS DURING RYANODINE RECEPTOR CHANNEL ADAPTATION. ((*A. Zahradníková*[a,b], *I. Györke*[a], *and S. Györke*[a])) [a]Department of Physiology, TTUHSC, Lubbock, TX 79430, [b]Laboratory of Electrophysiology, UMFG SAV, 833 34 Bratislava, Slovak Republic (Spon. by K.-H. Cheng)

To define the mechanism of ryanodine receptor (RyR) channel adaptation, we analysed single-channel activity of cardiac RyRs in response to rapid and sustained increases in $[Ca^{2+}]$, produced by flash-photolysis of caged Ca^{2+} (DM-nitrophen). Channel activity was recorded in consequtive 1-sec segments using a planar bilayer technique. The transient kinetics of channel activity during a $[Ca^{2+}]$ step (adaptation) was manifested by a decrease in open probability (P_o), frequency of channel openings (n_o), and average open time (t_o) during the consecutive segments. (1 sec each, Fig. 1, *left*). These changes were due to a decrease in the proportion of segments (Fig. 1, *right*) with high P_o and longer openings (H-mode), and increases in the proportion of segments with low P_o and shorter openings (L-mode) and the proportion of segments without openings (I-mode) during the course of adaptation. These results suggest that RyR adaptation can be explained by an initial prevalence of H-mode upon channel activation, followed by a slow transition into a steady-state mixture of all three modes of activity.

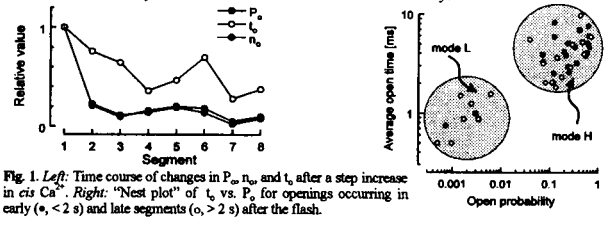

Fig. 1. *Left:* Time course of changes in P_o, n_o, and t_o after a step increase in *cis* Ca^{2+}. *Right:* "Nest plot" of t_o vs. P_o for openings occurring in early (•, < 2 s) and late segments (○, > 2 s) after the flash.

M-PM-B2

INHIBITION OF THE SKELETAL MUSCLE RYANODINE RECEPTOR CALCIUM RELEASE CHANNEL BY NITRIC OXIDE. ((*L.G. Mészáros*[1], *I. Minarovič*[1,2], *and A. Zahradníková*[1,2])) [1]Department of Physiology and Endocrinology, Medical College of Georgia, Augusta, GA 30912. [2]on leave from UMFG SAV, 833 34 Bratislava, Slovak Republic

We have found that NO donors (SNAP, S-nitroso-N-acetylpenicillamine; SIN-1, 3-morpholino-sydnonimine; SNP, sodium nitroprusside) decrease both the rate of skeletal muscle sarcoplasmic reticulum (SR) Ca^{2+} release and the open probability of single ryanodine receptor Ca^{2+} channels (RyRCs) in planar lipid bilayers (Fig. 1). These effects of NO donors were prevented by the NO-quencher hemoglobin (Hb) and reversed by 2-mercaptoethanol (2-ME). Ca^{2+} release asessed in skeletal muscle homogenates was also reduced (Fig. 2) by NO generated *in situ* from L-arginine (Arg) by endogenous NO-synthase, sensitive to nitro-L-arginine methylester (L-NAME). The effect of NO on the RyRC can in part explain the NO-induced depression of contractile force[1] in striated muscles and may represent an important feedback mechanism involving Ca-dependent activation of NO production and NO-evoked reduction of Ca^{2+} release from intracellular Ca^{2+} stores.

[1] L. Kobzik et al., *Nature* **372**: 546-548, 1994

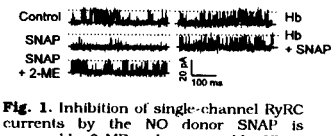

Fig. 1. Inhibition of single-channel RyRC currents by the NO donor SNAP is reversed by 2-ME and prevented by Hb.

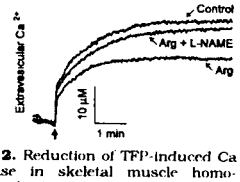

Fig. 2. Reduction of TFP-induced Ca release in skeletal muscle homogenate by Arg is reversed by L-NAME.

M-PM-B3

THE MECHANISM OF QUANTAL CALCIUM RELEASE FROM INTRACELLULAR STORES AND RELEASE CHANNEL ADAPTATION. László G. Mészáros, Alexandra Zahradnikova and Igor Minarovic. Department of. Physiol. Endocrinol., Medical College of Georgia, Augusta, GA 30912, USA.

The quantal kinetics of Ca^{2+} release from cerebellar microsomes and skeletal muscle sarcoplasmic reticulum (SR) vesicles mediated by the inositol 1,4,5-trisphosphate (IP_3) receptor (IRC) and the ryanodine receptor (RyRC), respectively, were analyzed on the basis of the assumption that both release channels spontaneously inactivate. The model we developed permitted us to determine relationships of 1) initial rate (v_o) and the rate of inactivation (v_i) of release flux *vs.* activating ligand concentrations (c_L) and 2) v_i *vs.* v_o. Since the ratio of v_i/v_o was found to decrease with increasing c_L and the results of IP_3 binding studies revealed the existence of a single class of non-cooperative sites (K_{deq}= 52 nM; Hill coeff.=1.1), a model which is based on the homotetrameric structure of the release channels is proposed to account for channel adaptation and thus for quantal Ca^{2+} release. According to this model, i) the release channels spontaneously inactivate (as shown in the scheme) and ii) while the C - I equilibrium shifts to the left, as the **ratio of ligand-occupied/ligand-free** monomers in the tetrameric units of the release channels is increase.

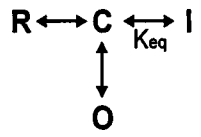

M-PM-B4

GATING OF THE Ca^{2+} RELEASE CHANNEL (CRC) BY ATP IS INHIBITED BY PROTEIN PHOSPHATASE 1 (PPT1) BUT NOT BY Mg^{2+} ((Alois Sonnleitner*, Sidney Fleischer*, Hansgeorg Schindler*)) *Institute for Biophysics, University of Linz, Austria; *Department of Molecular Biology, Vanderbilt University, Nashville,TN. USA 37235

Terminal cisternae vesicles of sarcoplasmic reticulum from skeletal muscle were incorporated into planar lipid bilayers. CRC gating by ATP (0.67 mM), in absence of Ca^{2+} (<1nM), was studied for treatments by protein kinase A (PKA) or phosphatase 1 (PPT1) and in the presence and absence of free Mg^{2+} (1mM). PPT1, PKA, and Mg^{2+} were directly applied to the bilayer using the microsyringe method. (Hain J., Nath, S., Mayrleitner M., Fleischer, S., and Schindler, H., 1994. Biophys. J. 67: 1823-1833) This permitted monitoring CRC activity (open probability) during phosphorylation/dephosphorylation cycles without perfusion steps. PKA treated channels (state p_{PKA}) were activated by ATP to high p_o values, while PPT1 treated channels (state d_{PPT1}) were not activatable by ATP. Opening and closing of channels during cycles of PKA and PPT1 applications provided evidence that the change of CRC activity is due to cyclic phosphorylation/dephosphorylation (cycles were:$p_{PKA} \rightarrow d_{PPT1} \rightarrow p_{PKA}$ and $d_{PPT1} \rightarrow p_{PKA} \rightarrow d_{PPT1}$). Free Mg^{2+} applied after each treatment, revealed that the activity of the CRC in both states, p_{PKA} and d_{PPT1} is not affected by 1mM free Mg^{2+} at free ATP of 0.67mM. Our results indicate that at low Ca^{2+} (nM) and in the presence of ATP (0.67mM), only phosphorylated CRC are active, whereas dephosphorylated CRC remain closed. ATP gating of CRC was independent of Mg^{2+} levels. (Supported by the Austrian Research Fond., project S6613-MED and NIH HL32711)

M-PM-B5

PHOSPHORYLATION OF THE RYANODINE RECEPTOR (RyR) MODULATES Ca^{2+} FLUXES IN SARCOPLASMIC RETICULUM (SR) FROM SKELETAL MUSCLE. ((J. Oliver McIntyre, Eunice Ogunbunmi, Sabine Rund, Christopher A. Adams and Sidney Fleischer)). *Dept. of Molecular. Biology., Vanderbilt Univ, Nashville, TN* 37235.

We previously reported that the RyR of terminal cisternae (TC) of SR can be phosphorylated in planer bilayers by protein kinase A (PKA) and Ca^{2+}/calmodulin-dependent protein kinase type II (CamKII) [Hain, et al, *Biophys. J.* 67, 1823-1833]. The phosphorylation was found to activate the RyR channel as measured in single channel measurements. Complementary experiments were carried out in TC. The stoichiometry of phosphorylation of the RyR was 1.9 and 0.9 by PKA and CamKII, resp.; phosphorylation resulted in a concomitant reduction in the net calcium loading rate of TC vesicles (3-fold and 2-fold, resp.)[Mayrleitner, et al *Cell Calcium* 18, 197-205]. We now report conditions to phosphorylate RyR-1 with PKA more selectively to give a stoichiometry of 0.7 ± 0.1 with essentially complete loss of ATP-dependent calcium loading by the TC. Ca^{2+} flux studies of TC can provide a macroscopic average of RyR-1 function; channel activation results in decreased net Ca^{2+} uptake by TC. With RyR-1 phosphorylated by PKA, Ca^{2+} uptake by TC was restored by closing the RyR channel with ruthenium red. We could not improve on the phosphorylation stoichiometry of RyR with CamKII (0.8 ± 0.2, 1mM Ca^{2+}). The sites of phosphorylation by PKA and CamKII are not susceptible to endogenous phosphatases under the conditions studied. We conclude that the skeletal muscle RyR in TC can be phosphorylated by either PKA or CamKII to a stoichiometry of about one ^{32}P per RyR channel (4RyR protomers) and that this phosphorylation acitivates the RyR channel in TC.(NIH HL 32711)

M-PM-B6

MUTATING A PORE REGION GLUTAMATE IN REPEAT III OF THE SKELETAL L-TYPE Ca^{2+} CHANNEL ABOLISHES Ca^{2+} PERMEATION BUT NOT E-C COUPLING. ((R. T. Dirksen and K. Beam)) Dept. Neurobiol. and Anat., CSU, Ft. Collins, CO 80523.

A glutamate in the pore region of repeat III of the cardiac L-type Ca^{2+} channel strongly influences ion selectivity (Yang, *et al.*, 1993). Upon expression in dysgenic myotubes, we compared the properties of this cardiac mutant channel (CEIIIK) with those of the analogously mutated skeletal L-channel (SkEIIIK). Expression of SkEIIIK, but not CEIIIK, restored E-C coupling. Both constructs produced predominantly outward whole-cell currents (extracellular: 145 mM TEA^+ and 10 mM Ca^{2+}; intracellular: 150 mM Cs^+). With CEIIIK, but not with SkEIIIK, small inward currents were present at negative voltages, indicating that this glutamate is even more essential for calcium permeation in the skeletal channel. As for the wild-type channels, CEIIIK current activated > 10-fold faster than SkEIIIK current (at +60 mV, CEIIIK: 3.7 ± 1.4 ms; SkEIIIK: 40.0 ± 2.6 ms). Immobilization-resistant charge movements were measured after block of ionic currents by 2 mM Cd^{2+} + 0.2 mM La^{3+}. For CEIIIK, Q_{off} was similar following either 20 or 200 ms test pulses. For SkEIIIK, repolarization following 200 ms depolarizations to potentials sufficient to activate ionic current resulted in a Q_{off} that was 22 ± 2.4% larger than Q_{off} following a 20 ms depolarization to the same potential. This time-dependent increase in Q_{off} associated with SkEIIIK suggests that the rate-limiting step in skeletal L-current activation involves a transition that is slow at positive potentials (where current activates slowly) and fast at negative potentials (where current deactivates rapidly). Supported by AR08243 (RD) and NS24444 (KB).

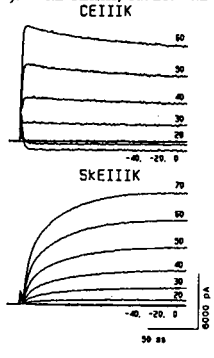

M-PM-B7

RESTORATION OF EXCITATION-CONTRACTION COUPLING AND SLOW CALCIUM CURRENT BY EXPRESSION OF RYANODINE RECEPTOR. ((J. Nakai[1], R.T. Dirksen[1], H.T. Nguyen[2], I.N. Pessah[3], K.G. Beam[1] and P.D. Allen[2,4])) 1. Colorado State Univ., 2. Boston Childrens Hospital, 3. Univ. of California-Davis, Sch. of Vet. Med. and 4. Brigham and Women's Hospital.

The skeletal muscle dihydropyridine receptor (DHPR) functions both as a voltage sensor for excitation-contraction (E-C) coupling and an L-type Ca^{2+} channel. The voltage sensor controls gating of the skeletal muscle ryanodine receptor (RyR-1) which is the Ca^{2+} release channel in the sarcoplasmic reticulum. If RyR-1 is directly coupled to the DHPR, then the interaction should be reciprocal and gating of the DHPR should also be influenced by RyR-1. To test the hypothesis, we analyzed the membrane currents and Ca^{2+} transients in dyspedic myotubes, which have a disrupted RyR-1 gene, using whole-cell patch clamp and Ca^{2+} indicator dye Fluo3. As previously reported, dyspedic myotubes both lack E-C coupling and show greatly reduced Ca^{2+} transients in response to RyR agonist. Additionally, L-type Ca^{2+} current density was reduced ~30-fold in dyspedic myotubes (0.6 ± 0.7 pA/pF) compared to that in normal myotubes (16.8 ± 4.3 pA/pF). When RyR-1 was expressed after nuclear injection of a RyR-1 cDNA, Ca^{2+} current returned towards normal (6.2 ± 2.5 pA/pF) and E-C coupling was restored. Measured immobilization-resistant charge movement for dyspedic and RyR-1 expressing dyspedic myotubes were 4.0 ± 1.4 nC/μF and 4.0 ± 1.5 nC/μF, respectively. These results suggest that the density of sarcolemmal DHPRs is similar in dyspedic and RyR-1 expressing myotubes. One interpretation of these results is that the presence of RyR-1 enhances the ability of DHPRs to function as Ca^{2+} channels. Supported by NIH (NS24444) and MDA.

M-PM-B8

INTER-SUBUNIT DISULFIDE FORMATION MAY EXPLAIN OXIDATIVE EFFECTS ON Ca^{2+} RELEASE CHANNEL FUNCTION. ((Bahman Aghdasi*, J.Z. Zhang*, Ken Slavik*, Michael B. Reid**, Susan L. Hamilton*.)) Department of Molecular Physiology and Biophysics*, & Department of Medicine**, Baylor College of Medicine, Houston, TX 77030.

Diamide, a thiol-oxidizing agent, and dithiothreitol (DTT), a thiol-reducing agent, were tested for effects on the skeletal muscle Ca^{2+} release channel. As observed by others (Zaidi *et al., J.Biol.Chem.264(36):21725-36,1989.* Boraso *et al. Am. J. Physiol. 267(3pt2):H1010-6, 1994*), oxidation of thiol(s) increases the probability of opening (P_o) of the channel and reduction decreases this probability. Consistent with this, diamide enhances and DTT inhibits [^{3}H]-ryanodine binding. To elucidate the mechanism of oxidation, both membrane and purified receptor were treated with diamide and run on SDS-polyacrylamide gels in both the absence and presence of DTT. Electrophoresis of diamide treated samples showed the formation of high molecular weight complexes which appear to arise from intersubunit crosslinks. To explore further the consequences of disulfide formation, we investigated the effects of the order of addition of ryanodine and diamide to the channel reconstituted into a planar lipid bilayer. If diamide is added first there is an increase in probability of opening and subsequent addition of ryanodine produces a typical ryanodine-modified channel with reduced conductance and high P_o. If, however, diamide is added to a ryanodine-modified channel, the conductance of the channel is increased from the subconductance state to almost a full conductance state. The P_o of the channel, however, remains at a value consistent with a ryanodine-modified channel. Similar results were obtained with purified ryanodine receptor. Our data suggest that diamide enhances channel activity through the formation of intersubunit crosslinks. Oxidation of the ryanodine modified channel with diamide may involve different crosslinks than those formed with diamide treatment of the unmodified channel. (Supported by NIH Grant 5RO1-AR41802-3.)

M-PM-B9

PROBING THE TERTIARY STRUCTURE OF RYANODINE RECEPTOR BY PROTEOLYSIS AND CROSSLINKING. ((Y. Wu, S. Dou, B. Aghdasi, and S. L. Hamilton)) Department of Molecular Physiology and Biophysics, Baylor College of Medicine, Houston, TX 77030.

The ryanodine receptor (RyR) proteolysed by endogenous and exogenous calpains has been isolated by sucrose gradient centrifugation and examined by western blot analysis using sequence-specific antibodies and anti-RyR polyclonal antibody. Unlike the trypsin cleaved complex which undergoes a shift from 30S to 14S, the calpain proteolytic complex shifts only from 30S to 28S. After the N-terminal 170kDa fragment is removed at the initial cleavage, the remaining 400kDa peptide is successively degraded by calpain. Antibody against the last 9 amino acids at the C-terminus of RyR revealed several fragments from 97kDa to 43kDa in the isolated 28S-30S complex. The 170kDa band is relatively stable and is degraded at a much slower rate than the 400kDa band. To investigate nearest neighbors, the proteolytic complex was treated with diamide, a thiol-oxidizing agent, and electrophoresed in two dimensions, reducing prior the second dimension. The N-terminal 170kDa fragment and the C-terminal fragments are shown to be involved in crosslinks, apparently forming disulfide bonds with like fragments of neighboring subunits. This result, together with our observation that diamide activates the channel, suggests that the formation of intersubunit crosslinks contributes to the activation of the channel and that these crosslinks occur between C-terminal (43kDa) fragments and/or between N-terminal (170kDa) fragments of the Ca^{2+} release channel monomers. (Supported by grants from MDA and NIH)

FOLDING AND SELF-ASSEMBLY: DYNAMICS AND THEORY

M-PM-C1

USING PHASE-PORTRAITS TO VISUALIZE SUB-STATES, SAMPLING, AND CHAOS IN PROTEIN DYNAMICS

((J. B. Clarage, T. D. Romo, B. K. Andrews, B. M. Pettitt†
G. N. Phillips Jr.,))
Keck Center for Computational Biology
(email: clarage@rice.edu, WWW http://www-bioc.rice.edu/~clarage/science/)

Making sense of a molecular dynamics simulation on a macromolecule entails simultaneously following the movements of thousands of atoms. The complexity of this task can be enormously reduced by treating the molecule as a dynamical system, evolving as a single point in a multi-dimensional phase space. Due to the number of degrees of freedom in a protein, such a global view of the dynamics cannot be directly visualized; however, judicious projections of the trajectory down to three dimensions results in an interpretable picture. Applied to myoglobin such portaits clearly show i) the rich population of local and global substates, ii) how solvent facilitates the transitions between these substates, thereby enhancing sampling, iii) protein dynamics is quite chaotic (Lyanupov exponent of 100fs), and iv) the available phase space for atomic motions is so large for proteins that two chemically identical molecules will live two dynamically distinct lives during their history in the cell.

(This work supported by NIH, NSF, The W.M. Keck Center for Computational Biology, and the Robert A. Welch Foundation.)

M-PM-C2

MOLECULAR DYNAMICS SIMULATION OF EQUILIBRIUM FOLDING AND UNFOLDING TRANSITIONS OF PROTEINS. ((Angel E. Garcia and Gerhard Hummer)) Theoretical Biology and Biophysics Group, Los Alamos National Laboratory, Los Alamos, NM 87545.

We study the equilibrium folding/unfolding transitions of a small protein, crambin, by means of molecular dynamics simulations at constant temperature. Configurations of the protein are sampled over a wide range of temperatures (300K to 900K). Simulations extend over periods of 1 to 4 nanoseconds for each temperature. Energy and structural parameters are analyzed using single and multiple histogram methods. These analyses show a transition from a compact folded state to a molten-globule-type state around 400K. We will discuss the methods and describe the structural features of the various states. Implications of these structures to a folding/unfolding pathway will be discussed.

M-PM-C3

MOLECULAR DYNAMICS SIMULATION OF SYNTHETIC PEPTIDE FOLDING ((Shen-Shu Sung and Xiong-Wu Wu)) Cleveland Clinic Foundation Research Institute, Cleveland OH 44195

Molecular dynamics simulations of helix folding of alanine-based synthetic peptides have been carried out at experimental temperature of 274 K. Including the average solvent effect in the potential functions greatly simplified the solvent calculation and made folding simulations (in tens of nanoseconds) feasible. The hydrophobic interaction was calculated based on the solvent accessible surface area. This solvent-referenced potential reduced the exaggerated energy changes of the *in vacuo* calculations and prevented the multiple-minima problem. From either an extended or a randomly generated conformation, the simulations approached a helix-coil equilibrium in about 3 nanoseconds. The calculated helical ratio of Ac-$(AAQAA)_3$Y-NH_2 was 47%, in good agreement with CD measurements (Scholtz et al. J. Am. Chem. Soc. 113:5102, 1991). A helical segment with frayed ends was the most stable conformation, but the hydrophobic interaction favored the compact, distorted helix-turn-helix conformations. The transition between the two types of conformations occurred in nanosecond time scale. The transient hydrogen bonds between the glutamine side chain and the backbone carbonyl group could reduce the free energy barrier of helix folding and unfolding. The substitution of a single alanine residue in the middle of the peptide with valine or glycine decreased the average helical ratio significantly, in agreement with experimental observations. In a molecular dynamics simulation with one layer of water molecules helix folding has also been observed.

M-PM-C4

CONSTRAINT DYNAMICS FOR MACROMOLECULES WITH RIGID FRAGMENTS ((Xiong-Wu Wu and Shen-Shu Sung)) The Cleveland Clinic Foundation, Research Institute, Cleveland OH 44195

The time scale a molecular dynamics simulation can reach is very limited because of the large number of degrees of freedom in a macromolecule and the short time step limited by the fastest motion, such as bond length and bond angle vibrations. Rigidifying the fragments containing only the fastest motion can reduce the number of degrees of freedom significantly and make a larger time step in molecular dynamic simulation possible. We developed a constraint dynamics algorithm for molecular dynamics simulation with rigid fragments. Each rigid fragment moves under the effect of the force field of the system and the constraint forces. The constraint forces acting on rigid fragments are calculated iteratively until all the constraint conditions are satisfied within a given tolerance at each time step. We applied the algorithm in molecular dynamics simulations of a series of polypeptides in which only ϕ, ψ dihedral angles were allowed to change. The parameters of the AMBER force field were used. Each peptide unit together with its covalently bonded carbon atoms, Cα-CONH-Cα, is treated as a rigid fragment. Each sidechain together with its covalently bonded atoms, N-Cα(Sidechain)-C, is treated as a different type of rigid fragment. The overlapping of the same atoms in different fragments is the constraint. The constraints were fulfilled using our algorithm during the movement at each time step. A time steps of 20 femtoseconds was used in our simulations. Energy conservation test in *NVE* ensemble showed a satisfactory result. Starting from the extended conformation, helix folding of several polypeptides has been simulated.

M-PM-C5

A SIMPLE TWO TERM ENERGY POTENTIAL CAN RECOGNIZE NATIVE STRUCTURES OF SMALL PROTEINS. ((K. Yue and K. A. Dill)) Department of Pharmaceutical Chemistry, Box 1204, University of California SF, CA 94143.

We report an energy potential and a search method that might be used for predicting protein structures. We use a united atom representation and discretized ϕ/ψ preferences. The energy potential has two terms: (1) Hydrophobic interaction is measured by non-polar surface area; (2) Polar group interaction is measured by the number of stand-alone H-bond donors (HBDs) and acceptors (HBAs) and the number of paired HBDs and HBAs *in the protein interior*. For average 3.2 to 4 ϕ/ψ choices per residue, we exhaustively enumerate conformations for crambin, avian pancreatic polypeptide, melittin and apamin. Native-like structures are among the conformations with the lowest energy. The native structures are 5-10% lower in energy than any enumerated conformation.

M-PM-C6

THE IMPACT OF DISCRETIZATION IN DECONVOLUTION ON THE ESTIMATION OF THE ANISOTROPY DECAY PARAMETERS. ((Ž. Bajzer, I. Penzar and F.G. Prendergast)) Mayo Foundation, Rochester, MN 55905.

Recently we have shown how more accurate discretization of convolution integrals substantially improves our ability to detect picosend lifetimes by time-correlated single photon counting technique [Bajzer et al., Biophys. J. 69(1995)1148-1161]. In the present study we investigate the impact of discretization of the convolution integral on parameter estimation for time-correlated single photon counting anysotropy decay measurements. In deconvolution based on the maximum likelihood method [Bajzer et al., Eur. Biophys. J. 20(1991)247-262] we considered the commonly used linear approximation, the quadratic approximation and cubic approximation within our general formula for discretization. To obtain anisotropy decay parameters we fitted the parallel and perpendicular time-dependent emission components simultaneously, in the sense of a global analysis. Accordingly, through one fitting procedure, both fluorescence decay lifetimes and rotational relaxation times were obtained.

To asses the accuracy of parameter estimation we performed Monte Carlo simulations. The results suggest that the zero-time anisotropy r(0) can be very accurately determined (within a few percent) by any of the considered discretization approximations. The impact of a discretization approximation on the estimation of rotational relaxation times is detectable, but less substantial than its impact on the estimation of fluorescenc lifetimes. However, this study does show that the quadratic and cubic approximations do provide the most accurate results. Supported by GM34847.

M-PM-C7

LINEAR MODEL PREDICTING NONIDEALITY OF MIXED AMINO ACID SOLUTIONS USING SOLUTE/SOLVENT INTERACTIONS. ((C.R. Keener, G.D. Fullerton and I.L. Cameron)) University of Texas Health Science Center at San Antonio, San Antonio, TX 78284.

A simple linear model is proposed for predicting the nonideality of a solution consisting of two amino acid monomers. The model is based on the theory that solution nonideality is due primarily to interactions between solute molecules and adjacent water molecules, with direct solute/solute interactions having an insignificant effect. The model is based on two characteristics of each solute: (1) the number of solute molecules in the solution and (2) the nonideality associated with each solute molecule. The nonideality is described by I_n, an empirically-derived parameter describing the perturbation number of water molecules per solute molecule. Using freezing point depression measurements, the colligative nonideality was measured for eight mixtures each consisting of two amino acid solutes. The measured data agree with the predicted values from the proposed model. The model has been extended to solutions consisting of more than two amino acid solutes:

$$I_{n(\text{avg})} = \sum_i w_i I_{ni}$$

where $I_{n(\text{avg})}$ is the nonideality of the solution, w_i is the fraction of solute molecules consisting of the ith solute and I_{ni} is the nonideality due to the ith solute. The agreement of the model with the data supports the hypothesis that nonideality is due primarily to solute/solvent interactions.

M-PM-C8

TOPOLOGY OF THE PAULING HEXAGON AND THE FUNCTIONAL INTERACTIONS OF PROTEINS. ((O. Gurel)) IBM Corp. & ((D. Gurel)) Touro College, New York, NY 10010.

It was proposed that a hexagon, formed by a sequence of seven (7) consecutive C_α with the amino acid residues along the backbone chain of the α-helical region of proteins, constitutes a basic communication element (Gurel, O., *Z. Naturforsch.* **1975**, *30c*, 843). This hexagon was recently named the *Pauling Hexagon*. Its *geometry*, a *Euclidean space*, is defined by the stereochemistry of the backbone. The *orientation* is superimposed by the hydrogen bonds of the backbone chain. The hydrogen bonds of the individual amino acid residues form the *topology* of the functional interaction space. This topological property makes the Pauling Hexagon a *topological unit subspace* of the *functional interaction space*. Thus, it is *topologically equivalent* in helical and non-helical regions of protein molecules. The hydrogen bond formations in the hexagons truncated by removing the end positions at the N- and C-termini of the helix are also determined. It is observed that such truncated hexagons correspond to the *consensus motifs* at the end domains of the α-helical regions of known protein sequences, observed by Huggins, M. L. (*Chem. Rev.* **1943**, *32*, 195) and Watson, H. C. (*Progress in Stereochemistry* **1969**, *4*, 299) and discussed recently by Harper, E. T. & Rose, G. D. (*Biochemistry* **1993**, *32*, 7605) and Aurora, R., Srinivasan, R. & Rose, G. D., (*Science* **1994**, *264*, 1126).

M-PM-C9

Protein Folding and Wring Resonances

J.Bohr[1], H. Bohr[2] and S. Brunak[2]

[1] Physics Department, Building 307, The Technical University of Denmark, DK-2800 Lyngby, Denmark.

[2] Center for Biological Sequence Analysis, Building 206 The Technical University of Denmark, DK-2800 Lyngby, Denmark.

The winding topology of the peptide chain of proteins is shown to have long range geometrical implications for the conformation of the backbone. Constraints of topological nature must therefore be obeyed during protein folding. A new type of long range excitations which involve a wringing of the backbone exist. A protein backbone of a given length can therfore resonate with molecular modes present in the cell. It is hypothesized that the folding of proteins occurs when the amplitude of a wring excitation becomes so large that it is energetically favorable to bend the backbone. Accordingly, the initiation of protein folding is a resonance phenomenon. The origin of the difficulties often encountered when a protein is expressed by recombinant DNA in a non native environment is discussed.

M-PM-C10

SELF-ORGANIZATION, ENTROPY AND ORDER IN EVOLUTION. ((J.S. Shiner)) Physiologisches Institut, Universität Bern, Bühlplatz 5, CH-3012 Bern, Switzerland.

Evolution may well be the ultimate example of self-organization in nature. Self-organization itself is intimately related to order, a central concept of biological thought, which in turn is related to entropy. P.T. Landsberg (In "On Self-Organization", R.K. Mishra et al. eds., Springer, Berlin, pp. 158-184, 1994) has referred to the "popular perception: self-organisation → greater order → lower entropy". However, he has also noted several times that the concomitant increase in entropy and disorder may not follow our intuition about disorder in growing systems, of which evolution is an example. This is the case since entropy is an extensive quantity and will increase with the size of the system, whereas what we perceive as order may also increase. Landsberg has proposed that disorder be defined as the actual entropy normalized to the maximum possible entropy for a given number of states. Order is then defined as 1 - disorder. We investigate the suitability of this definition as a measure of order in evolution. We calculate order as indicated by the number of distinct cell types throughout phylogeny using both the actual number of cell types and the number of cell types predicted by S. Kauffman's Boolean NK networks ("The Origins of Order", Oxford, 1993). Although we find that the order of even the simplest organisms is very high, we also find that order increases together with entropy throughout phylogeny. We conclude that Landsberg order may be one appropriate definition of order for self-organizing systems.

M-PM-D1

INCREASED EXPRESSION OF MYOSIN WITH INSERTION IN THE NH_2-TERMINAL REGION IN THE DISTRIBUTING (MUSCULAR) ARTERIES.

((Michael DiSanto, Ze Wang, and Samuel Chacko)) Department of Pathobiology, and Division of Urology, University of PA, Philadelphia, PA. (Spon. by N.R. Avadhani)

The myosin heavy chain (MHC)from visceral, but not the vascular, smooth muscle contains seven unique amino acids, encoded by an insert of 21 nucleotides in the 5'-terminal coding region near the 25-50- kDa junction which is close to the ATP-binding region (Babij, Kelly, and Periasamy, Proc. Natl. Acad. Sci., 88:10676, 1991). C.A. Kelly et al. (J. Biol. Chem., 268:12848, 1993) showed that the enzymatic activity of inserted myosin in visceral smooth muscle is higher than that of the aortic myosin, which is noninserted. Using reverse-transcriptase-PCR (RT-PCR), we demonstrate that, while abdominal aorta from rabbit consists almost entirely of MHC mRNA with no insert at the 5'-terminal coding region, the distributing arteries, that branch out at the bifurcation of the aorta (external iliac artery and its branches), begin to show MHC mRNA with the 21 nucleotide insert and the inserted mRNA transcript increases as they continue to become the saphenous arteries. The saphenous artery contains >95% inserted mRNA. The actin-activated ATPase activity of myosin from the distributing arteries is 2-fold higher than that of the myosin from aorta, indicating that the preponderance of the inserted myosin is associated with an increase in the actin-activated ATPase activity. Furthermore, the aorta contains both the 17 kDa light chain isoforms a&b, while the myosin from distributing arteries contains only the b isoform. Taken together, these data indicate that the smooth muscle cells from distributing arteries are similar to those of the visceral smooth muscle with respect to the smooth muscle isoform. Supported by NIH Grants DK39740 & DK47514.

M-PM-D2

FUNCTION OF THE 25/50 KDA LOOP OF THE MYOSIN II MOTOR.

((H.L. Sweeney, L. Faust, J.E. Smith, F. Brown, R.A. Milligan, J.R. Sellers and L.A. Stein))) University of Pennsylvania School of Medicine, Philadelphia, PA 19104; Scripps Research Institute, La Jolla,, CA 92037, NHLBI, Bethesda, MD 20892; and SUNY Stony Brook, Stony Brook, NY 11794.

As revealed by the X-ray crystal structure, the motor domain of myosin II contains a disordered loop near the nucleotide binding pocket. This loop forms the boundary between the 25 and 50 KDa proteolytic domains of the myosin motor, and is thus referred to as the 25/50 KDa loop. Using baculovirus/SF 9 cell expression of wild type and mutant chicken gizzard smooth muscle myosin S1 and HMM, we have assessed the function of this loop by measuring the rate of ADP release (via stopped flow light scattering measurements), the rate of *in vitro* motility and the steady state ATPase activity. All measured properties were effected by either deletion of the loop or chimeric loop substitutions, with loops derived from another myosin II (rat smooth SM1A, chicken fast skeletal or rat cardiac beta.). With the loop deleted, ADP release was slowed 5 fold. Chimeric loops gave intermediate values. Deletion or substitution of the loop also slowed ATPase activity and *in vitro* motility, but to differing extents relative to the effect on the ADP release rate. The alternative smooth (SM1A) loop was two-threefold slower than the gizzard loop both in terms of ADP release and *in vitro* motility. Using cryo-electron microscopy and helical image analysis, 3D maps of S1 with and without the 25/50 KDa loop were calculated. Difference maps allowed localization of the loop. We conclude that the function of this loop is to increase the rate of ADP dissociation from the nucleotide pocket. While different loops alter the rate to differing degrees, the loop is modulatory and is not the primary determinant of the ADP release rate and/or the speed of myosin movement.

M-PM-D3

COORDINATED ELECTRON PARAMAGNETIC RESONANCE AND X-RAY DIFFRACTION INVESTIGATION OF SPIN-LABELED SINGLE CRYSTALS OF TRUNCATED *DICTYOSTELIUM* MYOSIN.

((Edmund C. Howard, James B. Thoden, Ivan Rayment, and David D. Thomas)) University of Minnesota Medical School, Minneapolis, MN 55455 and University of Wisconsin-Madison, Madison, WI 53706.

We have obtained EPR spectra of single crystals of truncated *Dictyostelium discoideum* myosin II (S1Dc) with a BeF_x-trapped spiroketal ADP spin label, 2',3'-*O*-(1-oxy-2,2,6,6-tetramethyl-4-piperidylidene)ADP, and collected X-ray diffraction data from these crystals. The EPR spectra show the spin label to be very well ordered and immobilized at 4° C, while the X-ray diffraction data, collected at -160 °C, clearly show the spin label's position in the myosin molecule. This probe, with its restricted mobility relative to the ribose ring, is particularly useful for investigating the orientation and conformational freedom of the nucleotide during the myosin ATPase cycle, as well as the conformation of the nucleotide binding pocket.

M-PM-D4

OBSERVATION OF TWO-STEP BINDING OF MYOSIN-S1 TO ACTIN BY MILLI-SECOND TIME-RESOLVED ELECTRON CRYOMICROSCOY.

((Matthew Walker, John Trinick, and Howard White)). Bristol University Veterinary School, Langford, Bristol BS18 7DY, UK and Dept. of Biochemistry, Eastern Virginia Medical School, Norfolk, Virginia 23507.

We have used spray-mixing and electron-cryomicroscopy to observe rapid binding of myosin-S1 to actin. Droplets ~0.5 um in size containing myosin-S1 are sprayed onto a grid layered with a film of F-actin less than 0.1 um thick. The grid is then frozen by plunging it into liquid ethane. Improved control of the size and distribution of the spray is obtained by regulating the liquid input to the sprayer using a syringe pump driven by a microstepping motor. A 5-10 fold increase in the number of sub-micron droplets on the grid is obtained by placing an 8 kV potential between the nozzle of the sprayer and the grid. Air pistons are used for blotting and plunging the grid into the ethane. The timing of the syringe pump, blotting, spraying, high voltage, and grid descent are computer controlled. The length of reaction time is varied by controlling the length of time between spraying and freezing. Times of 5-50 msec are obtained by varying the velocity of the grid and the distance between spraying and freezing. For longer times the grid is stopped between spraying and freezing. In some of the micrographs of the hydrated specimens the binding of the S1 was disordered. The appearance seen is similar to that observed during steady-state ATP hydrolysis (Walker et al, Biophys. J. 66, 1563-1572) and a few milliseconds after spraying grids containing actomyosin-S1 with ATP (Walker et al, Biophys. J. 68, 87s-91s). In other regions of the grids the bound S1 has a similar appearance to the rigor conformation observed in the absence of ATP. This work is supported by HR40964 and MRC (UK).

M-PM-D5

CHARACTERIZATION OF THE BIOCHEMICAL KINETICS AND CELLULAR DYNAMICS OF *ACANTHAMOEBA* MYOSIN-I.

((E.M. Ostap and T.D. Pollard)) Department of Cell Biology and Anatomy, The Johns Hopkins University School of Medicine, Baltimore, MD 21205.

Acanthamoeba myosin-IA (MIA) and myosin-IB (MIB) are single-headed molecular motors postulated to be important for the movement of organelles and membranes along actin filaments. To better define the types of motility supported by MIA and MIB, we used fluorescence stopped-flow, cold-chase, and rapid-quench techniques to determine the rate constants for key steps on the MI ATPase pathway: ATP binding, ATP hydrolysis, actomyosin-I dissociation, phosphate release and ADP release. We also determined equilibrium constants for MI binding to actin filaments, ADP binding to actomyosin-I and ATP hydrolysis. These rate and equilibrium constants define an ATPase mechanism in which (1) actomyosin-I dissociation in the presence of ATP is very fast, (2) phosphate release is rate limiting and regulated by heavy-chain phosphorylation, (3) the predominant steady-state intermediates are in a rapid equilibrium between actin-bound and free states, and (4) ADP release is fast. During steady-state ATP hydrolysis, MI is weakly bound to actin filaments. The mechanism is similar to the ATPase mechanism of skeletal muscle myosin-II, and it is unlike that of the microtubule-based motor kinesin. Therefore, for MI to support processive motility, multiple MI molecules must be localized to a small region of a membrane or actin filament. This conclusion has important implications for the regulation of MI via localization through the unique MI tails. This is the first complete transient kinetic characterization of a member of the myosin superfamily, other than myosin-II. The similarity of the chemical mechanism to muscle myosin, suggests that (1) the common myosin ancestor (over 1 billion years ago) had this mechanism and (2) the rapid equilibrium of weakly bound intermediates is a fundamental feature of myosins that may be shared by other myosin families as well.

M-PM-D6

PEG EFFECTS ON MYOSIN STRUCTURE AND MgATP INTERACTIONS

((Stefan Highsmith, Roger Cooke*, Kelly Duignan, Kathy Franks-Shiba* & Joel Cohen)) UOP and *UCSF, San Francisco, CA

Polyethylene glycol (PEG) was used to probe hydration and structural changes that occur during ATP hydrolysis by skeletal muscle myosin subfragment-1 (S1). For up to 10 wt% concentrations of PEG-1000 to PEG-6000, there are no significant effects. S1 is not aggregated. Tryptophan fluorescence intensity is unchanged for S1 and S1.MgADP.P_i, consistent with no structural changes for those species. The quenching of bound ϵADP fluorescence by acrylamide is not changed, and the ADP-induced decrease in the fluorescence intensity of cys-707-acetamido-fluorescein-S1 is constant, indicating that the active site is not affected. The kinetic parameters Km, Vmax and the phosphate burst are not changed by PEG < 10 wt%, suggesting that the ATP binding, hydrolysis and product release steps do not involve significant changes in S1 hydration. These results suggest that the opening or closing of any large crevice in the S1 structure, which would require significant changes in hydration of S1, is not part of the ATP hydrolysis cycle.

PEG-3000/4000 in the 20 wt% range does cause structural changes in S1 and S1.nucleotide. S1 is aggregated and has ony 20% activity. The tryptophan fluorescence intensity is 50% of normal and increases only 12%, instead of 24%, when S1.MgADP.P_i formed. These data suggest that higher [PEG] dehydrates S1 and changes its conformation. This result is compatible with a crevice closure, but it does not appear to be the active site. MgADP binding is decreased. Acrylamide quenching of ϵADP is increased. The active site appears to be more open. Strikingly, aggregated S1.MgADP is strongly protected against cross-linking by p-phenylenedimaleimide. These results are not due to reduced diffusion. These data suggest that in 20 wt% PEG3000 the active site of the dehydrated S1 is more open and that the nucleotide-induced conformational change in the cys-697 to cys-707 region of S1 that occurs in solution is inhibited. (NIH grant PO1 AR 42895)

M-PM-D7

ATP CONSUMPTION IN DIFFERENT TYPES OF HUMAN SKELETAL MUSCLE FIBRES. ((G.J.M. Stienen, J.L. Kiers, R. Bottinelli* and C. Reggiani*)) Department of Physiology, Free University, Amsterdam, The Netherlands and the *Institute of Human Physiology, University of Pavia, Pavia, Italy.

The rate of myofibrillar ATP consumption and isometric tension (P_o) were determined in chemically skinned skeletal muscle fibres from human rectus abdominus and vastus lateralis muscle in the range from 12 - 30 °C. In each fibre, myosin heavy chain (MHC) isoforms were identified. ATP consumption was determined photometrically from the absorbance of NADH in a coupled enzyme assay at saturating [Ca^{2+}] (pCa 4.3). Type I, IIA, IIB and mixed IIA/B MHCs were resolved from single fibre segments by 6% SDS gel electrophoresis. The relative increase in ATPase activity for a 10°C temperature change (Q_{10}) was temperature independent and amounted to 2.59 ± 0.08. The temperature coefficient of P_o was smaller and decreased with temperature. In the range between 12 and 20 °C, where sufficient data were collected to allow a comparison between fibre types, no difference in Q_{10} of ATPase activity was found between fibre types. Force appeared to be more temperature sensitive in slow type I fibres than in fast type IIB containing fibres. From these measurements, estimates were obtained for the isometric rate of ATP consumption (A_o) and force development (F_o) at muscle temperature *in vivo* (35 °C). After correction for osmotic swelling occurring upon skinning the following values were obtained: Type I: F_o= 190 kN/m^2, A_o= 0.6 mM/s; type IIA: F_o= 230 kN/m^2, A_o= 1.6 mM/s; type IIA/B: F_o= 280 kN/m^2, A_o= 1.9 mM/s; type IIB: F_o= 280 kN/m^2, A_o= 2.5 mM/s.

M-PM-D8

Mutagenic Analysis of the Role of Hydrophobic Residues in the 340-350 Helix on Actin in Actomyosin Interactions

*Carl Miller, °Tim Doyle, #Elena Bobkova, °David Botstein and #Emil Reisler #Dep of Chem. and Biochem. and the Mol. Biol. Inst., UCLA, Los Angeles, CA 90095 and °Dep. of Genetics, Stanford Univ. School of Medicine, CA 94305.

Yeast actin mutants with alanines replacing I341 and I345 in the alpha helix 340-350 were studied to assess their role in interactions with myosin. Substitution of I345 with alanine had no significant effect on the strong binding to myosin and actomyosin ATPase. In contrast to that, substitution of I341 with alanine reduced the strong binding of actin to myosin subfragment-1 (S1) eight-fold compared to wild type actin, decreased the V_{max} of the actin-activated S1 ATPase four-fold, and did not change the K_m value. The I341A mutation decreased the fraction of actin filaments sliding in the *in vitro* motility assay (to 65%) and decreased their mean velocity (1.6 ± 0.1μm/s) relative to wild type filaments (95%, 2.6 ± 0.3μm/s). However, addition of 2.0 mM MgADP to the motility assay buffer induced a uniform movement of all the I341A filaments. The decrease in motility of the I341A actin filaments in the absence of ADP was attributed to a negative load slowing the mutant filaments and the smaller force produced with the I341A actin. The latter conclusion was confirmed by showing that a greater percentage of NEM-modified heavy meromyosin (external load) was required for arresting the motion of wild type actin in the *in vitro* motility assay than that needed for stopping the I341A filaments. These results are consistent with the involvement of I341 in the transition between weakly and strongly bound actomyosin states.

EXOCYTOSIS AND ENDOCYTOSIS

M-PM-E1

THE DIVALENT CATION RECEPTOR FOR RAPID ENDOCYTOSIS IN CHROMAFFIN CELLS IS CALMODULIN. ((C. R. Artalejo[1], A. Elhamdani[1], and H. C. Palfrey[2])). [1]Dept. Neurobiol. & Physiol., Northwestern Univ., Evanston, IL60208 & [2]Dept. Pharmacol. & Physiol. Scis., Univ. Chicago, Chicago, IL60637 (Spon: P. Loach).

Rapid endocytosis (RE) immediately follows exocytosis in adrenal chromaffin cells and is complete within 20 sec as revealed by capacitance measurements. RE is strictly dependent on Ca influx as substitution of external Ca by Ba or Sr, while supporting a normal exocytotic episode, blocks RE (Artalejo et al, PNAS 92, 8328, 1995). This suggests that the divalent cation receptors for RE and exocytosis are different molecules. We tested whether calmodulin (CaM) could be the divalent cation receptor for RE. Four independent methods were used: RE was inhibited by intracellular loading of either (i) anti-CaM antibodies or (ii) the organic CaM antagonist calmidazolium (10^{-7}M) or (iii) the potent anti-CaM peptide RS20 (0.2 μM); a randomer based on the RS20 sequence (XRS20, 20 μM) was ineffective, whereas another CaM antagonist peptide (CaM-KII (290-309)) also blocked RE. (iv) RE could be "rescued" in Ba- or Sr-containing media by intracellular loading of Mn (0.1 mM), a CaM-stimulatory cation; Mn had no effect on secretion. Ba and Sr are not inhibitors of RE as membrane recovery could be elicited in Ca-containing solutions in the presence of intracellular Ba or Sr (0.1 mM). None of the methods used to inhibit CaM had significant effects on exocytosis or Ca currents. The divalent cation specificity of exocytosis is Ca>Ba>Sr>>>Mn while that for RE is Ca>Mn>>>Ba,Sr; the latter agrees with the specificity of CaM while the former does not. Thus we conclude that CaM is the divalent cation receptor for RE but not exocytosis in calf adrenal chromaffin cells. (Supported by NIH and Sloan Foundation).

M-PM-E2

STIMULATION OF SECRETION FROM CHROMAFFIN CELLS BY MICROSECOND TONEBURSTS OF ULTRASOUND. ((I.M. Robinson, R.R. Kinnick, J.F. Greenleaf and J.M. Fernandez)) Mayo Clinic, Dept. of Physiol. & Biophys., Rochester, MN 55905.

In this study the secretory response of individual bovine adrenal chromaffin cells was monitored using amperometric carbon-fiber microelectrodes. Cells were stimulated by exposure to 20-100μs tonebursts of therapeutic levels of ultrasound (2-4x10^{5}Pa Peak pressure at 1MHz). Three types of secretory responses were observed: i) an almost instantaneous response, ii) a delayed release of catecholamines, or, iii) a series of "burst-like" secretory bouts. Fura-2 measurements of intracellular Ca^{2+} concentrations showed that the release of catecholamines was accompanied by an increase in the intracellular Ca^{2+} concentration. The burst-like secretory events coincided with oscillations in intracellular Ca^{2+} concentrations. In the absence of extracellular Ca^{2+} secretory responses were not evoked showing that Ca^{2+} entry was necessary to elicit catecholamine release. The release of catecholamines from a single vesicle generates a current spike in the amperometric recording. Many of these spikes are preceded by a "foot". Following ultrasound stimulation, signals with an amplitude similar to these feet were recorded that were not followed by a spike. It is likely that these events result from the transient fusion of a secretory vesicle with the plasma membrane. Possible mechanisms of ultrasound induced Ca^{2+} entry into the cell are discussed. These results could help to explain some of the poorly understood mechanisms of action of therapeutic ultrasound.

M-PM-E3

EVIDENCE FOR ENDOCYTOSIS TRIGGERED BY EXOCYTOSIS OF SINGLE VESICLES IN HUMAN NEUTROPHILS FROM CAPACITANCE MEASUREMENTS. ((Karsten Lollike, Niels Borregaard, and Manfred Lindau*)).The Granulocyte Res. Lab., The Finsen Center, Rigshospitalet, DK-2100 Copenhagen, Denmark & *Dept. Molecular Cell Res., MPI f. Medical Research, D-69120 Heidelberg, Germany.

In cell-attached capacitance measurements exocytotic capacitance steps as small as 0.1 fF can be resolved [Lollike et al. (1995) JCB 129:99]. Most steps corresponding to the known vesicles/granules of the human neutrophil were seen with staircase appearance, but some fusion events were more complicated. Occasionally an individual vesicle flickered repeatedly, without undergoing full incorporation into the plasma membrane. In these multiple flickers the mean transient pore conductance was 474 pS and never exceeded 1nS. The on- and off-steps had the same size indicating that no net membrane transfer occurred during flicker, in contrast to what has previously been observed in mast cells [Monck et al. (1990) PNAS 87:7804]. In other cases single fusion events were followed by a single capacitance decrease which was usually smaller than the increase indicating net membrane transfer from the vesicle to the plasma membrane. In many cases the increase and decrease could be resolved in time. The changes in capacitance and conductance trace indicated that exocytosis occurred by opening of a fusion pore in a single vesicle. The decrease, however, was apparently continuous and started only when the pore conductance was too large to be resolved, sometimes larger than 2 nS. These results suggest a mechanism of endocytosis of several small vesicles (<100 nm) triggered by exocytosis and full fusion of a single much larger vesicle. Although the neutrophil is a short lived cell without the capability to reform exocytosed granules, exocytosis-triggered endocytosis might serve the function of recycling proteins essential for the fusion process.

M-PM-E4

PATCH-AMPEROMETRY: A NEW TECHNIQUE FOR STUDYING THE DYNAMICS OF VESICLE FUSION AND RELEASE DURING EXOCYTOSIS OF SMALL VESICLES. (M. Lindau[1] and G. Alvarez de Toledo[2]). [1]MPI f. med. Forschung, D-69120 Heidelberg, Germany [2]Dpto. Fisiología Médica y Biofísica. Universidad de Sevilla. 41009 Sevilla, Spain.

Cell attached measurements of membrane capacitance allow to resolve fusion of single secretory vesicles and granules with diameters approaching the size of small synaptic vesicles (Marty and Neher, *PNAS* 79, 6712, 1982, Lollike et al., *J.Cell Biol.*129, 99,1995). We combined this technique with amperometry to measure simultaneously the dynamics of release during exocytosis of small vesicles by inserting a polyethylene-coated carbon fibre electrode (6 μm diameter) into a patch pipette. A holder with two connectors was designed to record simultaneously the pipette current and the oxidation current from the carbon fibre with two different patch clamp amplifiers. To reduce noise, and for proper grounding of the carbon fibre in cell attached configuration, the pipette electrode was connected to ground. The command voltage used for capacitance measurements was applied to the bath electrode and the potential of the carbon fibre was set to +700-900 mV. Human neutrophils and chromaffin cells were used to test this new method. Ionomycin induced exocytosis in human neutrophils and produced large (>400 pA) oxidation currents at the amperometric detector, with fast rising and falling phases. The time integral of this signal paralleled the capacitance increase measured in these cells, suggesting that the amperometric signals reflect secretion into the patch pipette. However, O^{2-} generation by a respiratory burst may also contribute to the oxidation current. Experiments done with chromaffin cells revealed amperometric transients which resembled those previously measured with standard techniques including the frequent occurence of an amperometric foot. We demonstrate directly the relation between fusion and catecholamine release from single chromaffin granules.

M-PM-E5

KINETICS OF THE RELEASE OF SEROTONIN FROM ISOLATED SECRETORY GRANULES. ((P. Marszalek, B. Farrell, and J. Fernandez.)) Dept. of Physiol. and Biophys. Mayo Clinic, Rochester, MN 55905.

The release of secretory products is generally monitored from cells undergoing exocytosis. Since this system is complex and difficult to model we developed a method for measuring the release directly from isolated intact granules of the beige mast cell that combines electroporation of the granule membrane with amperometric detection of serotonin (5HT). A single secretory granule bathed in an electrolyte is placed between two platinum electrodes (distance ~ 100 μm) and is positioned adjacent (< 1 μm) to a carbon fiber microelectrode. A short (~30μs) high intensity voltage pulse (electric field of: ~5 kV/cm) is delivered to the electrodes which disintegrates the granule membrane and triggers the release of secretory products. Serotonin is oxidized at the carbon electrode (at overpotential of 650 mV) and this amperometric signal exhibits a spike-like time course. We find that the half-time ($t_{1/2}$) of the amperometric spike is related to the size of the granule by: $t_{1/2} \propto r^2$ where r is the radius of the granule. We use the expression: $t_{1/2} \propto r^2/D$ which describes the kinetics of ion exchange within a spherical particle to calculate the diffusion coefficient (D) of serotonin within the granular matrix. When granules were bathed in saline containing NaCl (150 mM, pH 7.2) we found D_{5HT} to be: ~ 10^{-8} cm^2/sec which is ~ three orders of magnitude less than the bulk value. Rapid swelling (3-5 fold increase in the granule volume) was observed during this release. In contrast, there was no apparent volume change in histamine dihydrochloride (100mM, pH 4.5 divalent cation) and the release was slightly slower. In $LaCl_3$ (88 mM, pH 7.2) there was a 2-10 fold increase in the time of release and 10-20% decrease in the granular volume. The observation that the external cation affects release strongly suggests that serotonin is released from the charged gel matrix by ion-exchange. We discuss the implications of the low diffusion coefficient (D_{5HT}) and hypothesize that an ion-exchange mechanism regulates exocytotic release.

M-PM-E6

USE OF THE ATOMIC FORCE MICROSCOPE (AFM) TO STUDY THE STORAGE OF HISTAMINE IN MAST CELL SECRETORY GRANULES.
((V. Parpura and J. M. Fernandez)) Mayo Clinic, Rochester, MN 55905.

Secretory products are stored in secretory granules and are released upon exocytosis. Two hypothesis implicated in the storage mechanism of transmitters are: (i) precipitation of transmitter in the lumen of the granule i.e. formation of a salt and (ii) electrostatic binding of transmitter to a charged gel matrix. In giant Beige mast cell granules (radius ~ 2 μm) there is much evidence to support hypothesis (ii). To investigate the storage of transmitters in normal mast cell granules (submicrometer size) we employed the AFM. Isolated granules were stripped of their membranes (Triton-X100; 0.01% for 5 min.) and then imaged with the AFM in a solution containing histamine dihydrochloride (100 mM; pH=3.5). We found the shape of the granular matrix to be spherical with an average height of 477 ± 8 nm (n = 335). To measure changes in the height caused by swelling of the granular matrix in various electrolytes we performed a series of force-distance curves. Changing the electrolyte from histamine dihydrochloride to sodium chloride (135 mM; pH=7.4) caused the matrix to swell as monitored by a change in the height (from 377 ± 32 nm in histamine to 677 ± 52 nm in sodium; n=12, $p<0.001$) and it returned to its original size after perfusion with histamine solution. This finding shows that histamine can be exchanged by other cations; it is bound electrostatically to a charged matrix and not stored as a salt. We also found that the swelling of the matrix decreased with an increase in the valency ($Na^+ > Ca^{2+} > La^{3+}$) of the external cation which is consistent with hypothesis (ii). In addition, force-indentation curves were employed to calculate the elastic (Young's) modulus of the matrices and range from 22.7 kPa in NaCl to 2.48 MPa in $LaCl_3$. These values are similar to those obtained for gelatin under various degrees of swelling (20 kPa - 1.8 MPa; Radmacher et al., 1995 *Biophys J.* 69: 264-270). We are currently examining the possibility that neurotransmitters are stored electrostatically in other secretory granules and synaptic vesicles.

M-PM-E7

BALLOON PATCH CLAMP, A NEW CONFIGURATION TO STUDY EXOCYTOSIS ((C. Solsona* and J. Fernandez)) Mayo Clinic, Rochester, MN and *Univ. of Barcelona, Barcelona, Spain.

We have found that patch clamped mast cells can be inflated by 4.3 ± 1.7 (n=14) times their original volume by applying a pressure equivalent to 5-15 cm H_2O to the interior of the patch pipette. Inflation does not cause changes in the pipette access resistance or in the cell membrane conductance and only causes a small reversible change in the cell membrane capacitance [36 ± 5 fF/cm H_2O]. The additional volume of the cell is entirely made of pipette solution, thus, an inflated cell is unambiguously perfused with the desired solutes. Mast cells inflated with solutions containing GTPγS (5 μM), did not degranulate while inflated. However, within minutes (1-3) of returning the pressure to 0 cm H_2O, the cell returned to its normal size and appearance and at this point, they degranulated completely (n=14). Exocytotic degranulation was followed with patch-clamp-capacitance techniques. A mast cell can remain inflated for more than 60 minutes and still readily degranulate upon returning to its normal size. We interpret these observations as an indication that inflated mast cells reversibly disassemble the structures that regulate exocytotic fusion. Upon returning to its normal size, the cell cytosol reassembles the fusion pore scaffolds and allows exocytosis to proceed. Reassembly of the fusion pore can be prevented by inflating the cells with solutions containing the protease pronase, which completely blocked exocytosis (n=5).

The balloon-patch-clamp technique allows for the certain perfusion of the cell's cytosol while holding the cell inactive for long periods of time. This technique can be used to introduce recombinant proteins and antibodies into the cytosol for up to 60 minutes before allowing the cell to degranulate.

M-PM-E8

TRANSIENT PORES IN FUSION OF LIPID VESICLES WITH PLANAR LIPID MEMBRANE. ((A. N. Chanturiya, J. Zimmerberg and L. V. Chernomordik)) LTPB, NICHD, NIH, Bethesda, MD 20892.

Giant unilamellar liposomes were added to planar lipid membranes (BLM) in the presence of calcium ions. Liposomes were formed with fluorescent lipid and nystatin channels in membranes and water soluble dye (calcein) inside, both dyes at a self-quenched concentration. Liposomes adherent to the BLM were observed as bright circular spots that moved when the solution was stirred but did not leave the plane of the membrane. With an osmotic gradient across the vesicle membrane, both complete fusion of the liposomes with the BLM (membrane dye transfer, release of water soluble dye and step-like increase of the planar membrane conductance) and hemifusion (membrane dye transfer only) were observed. Surprisingly, in many cases, release of vesicle internal content was not accompanied by large conductance steps but rather was associated with much smaller spikes of transmembrane current with highly variable amplitude and lifetime (30-800 pS; 50-1500 μs). This transient fusion pore formation was often preceded by membrane hemifusion and followed by complete fusion of liposome with BLM. The same phenomena (except complete fusion) was observed with liposomes osmotically balanced with external buffer. Thus, vesicle/planar bilayer fusion involves hemifusion and flickering of fusion pores, both stages reported earlier for protein mediated biological fusion.

TRANSMEMBRANE SIGNALING - MONOVALENT CATIONS

M-PM-F1

Scanning cysteine accessibility mutagenesis implicates both minK and a non-minK protein in pore formation.
((Kwok-Keung Tai, Ke-Wei Wang and Steve A. N. Goldstein)) Departments of Pediatrics and Cellular and Molecular Physiology, Boyer Center for Molecular Medicine, Yale University School of Medicine, New Haven, CT. 06536.

To identify minK residues which might contribute to a pore, we screened for blockade by two sulfhydryl-specific agents, methanethiosulfonate ethylsulfonate (MTSES) and ethylamine (MTSEA). Consecutive residues were studied in a minK region proposed to cross from the extracellular solution into the membrane using two-electrode voltage clamp and oocyte expression. Neither wild-type nor C107A-minK, in which the single natural cysteine is mutated to alanine, are affected by exposure to 10 mM MTSES. However, when residues 42 to 55 are mutated individually to cysteine, 3 sites render minK sensitive to irreversible block by MTSES: 44, 45 and 47. Cysteine substitution at other positions produces channels that exhibit wild-type K^+-selectivity, gating and insensitivity to MTSES. Blocking kinetics can be studied by abrupt exposure of oocytes to the agents. Varying test pulse duration, interpulse duration and command voltage has no effect on the time-course or magnitude of MTSES block of A45C-minK channels. This suggests that position 45 is exposed to the external aqueous milieu in both open and closed states and occupies a position superficial to the transmembrane electric field. MTSES modification of A45C-minK does not alter gating kinetics which suggests that block is by direct pore occlusion and not via allosteric effects on protein conformation. These results support the notion that minK position 45 is exposed in an external pore vestibule. Unlike MTSES, MTSEA irreversibly blocks both wild-type and cysteine-free C107A-minK channels potently. This argues strongly for the involvement of a cysteine-bearing, non-minK protein, together with minK, in pore formation.

M-PM-F2

TEA and MTSES interact in a minK K^+ channel vestibule
((Ke-Wei Wang, Kwok-Keung Tai and Steve A. N. Goldstein)) Departments of Pediatrics and Cellular and Molecular Physiology, Boyer Center for Molecular Medicine, Yale University School of Medicine, New Haven, CT. 06536.

Study of minK positions 42 to 55 supports the idea that this region lines an external pore vestibule. We find that: (1) binding site determinants for methanethiosulfonate ethylsulfonate (MTSES) and tetraethylammmonium (TEA) overlap in this region. Mutation to cysteine of positions 44, 45 and 47 render channels' sensitive to MTSES whereas 46, 47, 48 and 55 lower TEA affinity 25 to 120%. (2) MTSES and TEA interact negatively. When A45C-minK is blocked first by TEA and then abruptly exposed to MTSES (in the continued presence of TEA), the rate of irreversible MTSES block is slowed. As TEA dose increases, the time-course of MTSES block increases linearly while its final magnitude is unchanged. (3) TEA block appears to be by direct pore occlusion. First, TEA block is voltage-sensitive, acting as if it penetrates the transmembrane field to reach its minK receptor site ($z\delta$ ~ 0.15). Second, TEA block is sensitive to K^+ ions on the opposite side the membrane. Injection of 5 to 20 nmol KCl into oocytes expressing minK decreases external TEA affinity in a linearly dose-dependent fashion. RbCl and CsCl have similar effects while NaCl is inactive. Concordant with the idea that this represents entry of internal permeant ions into the conduction pathway and subsequent destabilization of the external pore blocker (i.e., "knock-off"), each cation decreases TEA affinity according to its relative permeability through open minK channels. These findings support the thesis that TEA and MTSES bind at interacting sites in an outer channel vestibule and that minK residues contribute directly to these sites. That internal permeant cations alter block by external TEA argues that, despite extremely small estimates for unitary conductance, minK forms an aqueous ion conduction pathway through the membrane.

M-PM-F3

IDENTIFICATION, EXPRESSION, AND EVOLUTIONARY SIGNIFICANCE OF A MEMBER OF A NOVEL CLASS OF K CHANNELS CONTAINING TWO P-REGIONS. ((W. J. Joiner, K. A. Ketchum, A. M. Quinn, A. J. Sellers, S. A. N. Goldstein, and L. K. Kaczmarek)) Departments of Cellular and Molecular Physiology, Pharmacology, and Pediatrics, Yale University School of Medicine, New Haven, CT 06520. (Sponsored by J. Howe).

Together, the P domain and part of the hydrophobic region immediately following it (S6 or M2) comprise the most highly conserved stretch of primary sequence in K channels. Searching multiple sequence databases using this region, which we call the core sequence, allowed us to identify many potential channel genes. Using this strategy, we obtained the full-length sequence of a gene from *Saccharomyces cerevisiae* encoding a novel K channel polypeptide with two P domains (Nature 376: 690-5, 1995). We named this gene TOK1, for *T*wo P-region-containing *O*utwardly-rectifying *K* channel. Depolarization of *Xenopus* oocytes injected with RNA derived from a PCR product of this gene elicited outward currents using two-electrode voltage-clamp. Interestingly, two kinetically distinct components were observed during activation. It is unclear at present whether these are indicative of a double-barrelled structure or whether both P regions line the same conduction pathway and together are capable of being gated by multiple activation pathways. Using the core sequence of known ion channels and additional, putative channels we identified, we also contructed a phylogenetic tree. Our results indicate that TOK1 is a member of a novel class of ion channels that is likely to share a prokaryotic ancestor with other classes of eukaryotic K channels.

M-PM-F4

VOLTAGE- AND G PROTEIN-DEPENDENT PROPERTIES OF MUSCARINIC RECEPTOR CATIONIC CURRENT IN GUINEA-PIG ILEUM. ((A.V. Zholos and T.B. Bolton)) Department of Pharmacology & Clinical Pharmacology, St. George's Hospital Medical School, London SW17 0RE, U.K.

Cationic current (I_{cat}) in single ileal smooth muscle cells produced by activating muscarinic receptors with carbachol or by dialysing cells with GTPγS has been studied using patch-clamp recording techniques. In both cases amplitude, kinetic and voltage-dependent properties of I_{cat} were similar. Relaxation kinetics was studied by stepping from -40 to -120 mV; I_{cat} increased instantaneously indicating a linear instantaneous I-V relationship and then decayed to a smaller steady-state value with a mean τ of 173±6 ms (n=154) in keeping with its U-shaped steady-state I-V relationship. Single channel conductance was 30 pS and did not depend on the membrane potential whereas the open probability decreased with hyperpolarization, thus explaining the sigmoidal Boltzmann-type activation curve and reduction in τ upon stepping to progressively more negative potentials. At the same test potential, τ was affected by changing the level of G protein activation such as by increasing fractional receptor occupancy by increasing agonist concentration or applying intracellularly GTP or GTPγS. In these cases, τ increased and a parallel negative shift of the activation curve on the voltage axis was observed. Receptor desensitization or GDPβS application had opposite effects. These results can be explained by assuming that 'efficacy' of channel opening (E=β/α, where β and α are voltage-dependent opening and closing rate constants) depends on both membrane potential and activated G protein subunit concentration. Calculations based on τ and steady-state activation measurements show that, for example, increasing agonist concentration from 3 to 300 μM resulted in an increase in E from 0.07 to 0.39.

M-PM-F5

ASSOCIATION OF G PROTEIN βγ-SUBUNITS WITH CELL MEMBRANE IS NECESSARY FOR ACTIVATING G PROTEIN-COUPLED INWARD RECTIFIER (K_{ir} (G)) IN BRAIN NEURONS. ((Y. Nakajima, S. Nakajima, and T. Kozasa)) Dept. of Anat. and Cell Biol., Dept. of Pharmacol., Univ. of Illinois at Chicago, Chicago, IL 60612 and Dept. of Pharmacol., Univ. of Texas Southwestern Medical Center, Dallas, TX 75235.

In cultured noradrenergic neurons from the rat locus coeruleus, we previously recorded using inside-out patches the single channel activity of K_{ir} (G) induced by somatostatin (Grigg et al., J. Neurophysiol., in press). We now report that in these neurons, application of recombinant G protein $\beta_1\gamma_2$-subunits (30 nM) to the cytoplasmic side induced single channel activity similar to the somatostatin-induced K_{ir} (G) (32 pS; -97 or -100 mV; $[K]_o$ = 156 mM; $[K]_i$ = 159 mM). In contrast, recombinant GTPγS-activated $G_{i2}\alpha$ (100 nM) did not activate the K_{ir} (G). Further, we tested a mutated γ_2-subunit in which the cysteine residue fourth from the carboxyl terminus was replaced by serine (γ_2C68S). This mutation is known to prevent prenylation of the γ_2-subunit. $\beta_1\gamma_2$C68S, unlike the wild-type $\beta_1\gamma_2$, does not effect adenylyl cyclases (Iñiguez-Lluhi et al., J. Biol. Chem., 1992). We found that $\beta_1\gamma_2$C68S (30 nM or 150 nM) failed to activate the brain K_{ir}(G) channel, suggesting that prenylation of the γ-subunit is necessary for the interaction of the βγ-subunits with the K_{ir}(G) channel. Prenylation of γ-subunits is important for the association of G proteins with the cell membrane (Muntz et al., Mol. Biol. Cell, 1992). Thus, our results suggest that the association of βγ-subunits with the cell membrane is a prerequisite for activating K_{ir}(G) channels. Supported by NIH grant AG06093.

M-PM-F6

ANTAGONISTIC MODULATION OF THE INWARD RECTIFIER K^+ CHANNEL, GIRK, BY α AND βγ SUBUNITS OF G PROTEINS. ((Wolfgang Schreibmayer[†], Carmen W. Dessauer [§], Dimitry Vorobiov[†], Alfred G. Gilman [§], Henry A. Lester[¶], Norman Davidson[¶], Nathan Dascal[†])). [†]School of Medicine, Tel Aviv University, Israel; [‡]Institut für Medizinische Physik und Biophysik, Universität Graz, Austria; [§]University of Texas, Southwestern Medical School, Dallas, TX, USA; [¶]Division of Biology, California Institute of Technology, Pasadena, CA, USA.

Several protein-coupled neurotransmitter receptors activate an inwardly rectifying "muscarinic" K^+ channel, GIRK, slowing the heartbeat and decreasing excitability of neuronal cells. Although previously both G_α and $G_{\beta\gamma}$ subunits of G proteins have been implicated in channel activation, recent studies attribute this role to $G_{\beta\gamma}$ that acts in a membrane-delimited fashion, probably by a direct binding to the channel protein. We show that free GTPγS-activated $G_{\alpha i1}$, but not $G_{\alpha i2}$ or $G_{\alpha i3}$, potently inhibits $G_{\beta 1\gamma 2}$-induced GIRK activity in excised membrane patches of *Xenopus* oocytes expressing the GIRK. High-affinity but partial inhibition is produced by $G_{\alpha s}$ and $G_{\alpha o}$. $G_{\alpha i1}$ also inhibits $G_{\beta 1\gamma 2}$-activated GIRK in atrial myocytes. The whole-cell acetylcholine (ACh)-evoked GIRK1 current, I_{ACh}, is significantly increased by an oligonucleotide against $G_{\alpha i1}$, but not $G_{\alpha i3}$, $G_{\alpha o}$, $G_{\alpha s}$ or $G_{\alpha q}$. Antagonistic interactions between G_α and $G_{\beta\gamma}$ may take part in determining specificity of G protein coupling to GIRK. Inhibition of GIRK by G protein-coupled receptors may be important in cardiac and brain physiology.

M-PM-F7

PROTEIN KINASE C REGULATES K_V1.3 CURRENT IN HUMAN T LYMPHOCYTES. ((L.C. SCHLICHTER and I. CHUNG)) U. of Toronto and Toronto Hospital, Ontario, CAN. M5T 2S8.

The voltage-gated potassium channel, K_V1.3, is expressed in human T lymphocytes, where its function is necessary for cell proliferation. K_V1.3 contains phosphorylation sites for protein kinase C (PKC), which is involved in T cell activation but little is known about the consequences of such phosphorylation for K_V1.3 channel function. We find that native K_V1.3 current in human T lymphocytes is regulated by cytoplasmic ATP and by PKC. ATP addition shifted the voltage dependence of activation by +6 mV and inactivation by +20 mV (i.e. towards more depolarized potentials) with a consequent increase in 'window current' (area under the crossover of the Boltzmann relations). ATP depletion by 'death brew' (2-deoxyglucose, adenylylimidodiphosphate, CCCP) reduced the K^+ conductance (G_K) by 41% and shifted inactivation by -7 mV. The PKC activator, 4-β phorbol 12,13-dibutyrate (4-βPDBu) increased G_K by 70% and shifted activation by +7 mV and inactivation by +9 mV. In contrast, extracellular addition of the membrane-permeant diacylglycerol analogue, 1,2-dioctanoyl-sn-glycerol (diC_8), caused an artefactual decrease in G_K via a process that resembled fast current inactivation, but was rapidly reversed by competition with an exogenous protein, human serum albumen. The contrasting effects of 4-βPDBu and diC_8 on K_V1.3 current correlated well with outcomes of functional studies of Ca^{2+} signalling and T cell proliferation. That is, 4-βPDBu enhanced T cell function, whereas diC_8 inhibited it. PKC inhibitory peptides added to the pipette reduced G_K by 40% (pseudosubstrate peptide) and 35% (substrate peptide). Calphostin C, a specific PKC inhibitor, when added to the bath, abolished the K_V1.3 current in a dose- and light-dependent manner. Hence, PKC both maintains and can further enhance K_V1.3 channel activity, especially at physiologically relevant membrane potentials. (Supported by MRC, OGS)

M-PM-F8

Monovalent cation permeation through stores-dependent Ca^{2+} channels (Icrac) in Jurkat T lymphocytes. ((Albrecht Lepple-Wienhues and Michael D. Cahalan)) Department of Physiology and Biophysics, UC Irvine, CA 92717. (Spon. by Nancy Allbritton)

Whole-cell membrane currents were recorded from Jurkat T lymphocytes using an internal Cs^+-aspartate solution buffered to 5 nM $[Ca^{2+}]_i$. Icrac channels were activated by passive store depletion or 10 μM inositol 1,4,5-trisphosphate, yielding a Ca^{2+} selective inward current.

When external free Ca^{2+} ($[Ca^{2+}]_e$) was reduced to micromolar levels in the absence of Mg^{2+}, the inward current at -20 mV first decreased and then increased 10-fold within 150 ms, accompanied by visibly enhanced current noise. Thereafter, the current declined slowly (τ=5 s). No conductance increase was seen when $[Ca^{2+}]_e$ was reduced before activation of Icrac. With Na^+ outside and Cs^+ inside, the current rectified inwardly without apparent reversal below 40 mV. The sequence of permeability determined from the inward current at -80 mV was $Na^+ > Li^+ = K^+ > Rb^+ >> Cs^+$. Unitary inward conductance of the Na^+ current was ≈2 pS, estimated from the ratios $\Delta\sigma^2/\Delta$ Imean at -20 and -60 mV. External divalent cations blocked the Na^+ current reversibly with IC_{50} values of $\approx 10^{-5}$ (Ca^{2+}) and $\approx 10^{-4}$ M (Mg^{2+}).

We conclude that Icrac channels become permeant to monovalent cations at low levels of external divalent ions. In contrast to voltage-activated Ca^{2+} channels, the monovalent conductance is highly selective for Na^+ over Cs^+, pointing to a different structure of the pore region in this channel type. Na^+ currents through Icrac channels provide a means to study channel characteristics in an amplified current model.

Supported by NIH grant NS14609 and DFG Le792/2-1.

M-PM-G1

TIME-RESOLVED X-RAY SPECTROSCOPY OF HEMEPROTEINS : NOVEL METHODS OF DATA ACQUISITION AND ANALYSIS APPLIED TO MBCO RELAXATION PHENOMENA ((M.R. Chance, A. Xie, L.M. Miller, R.F. Fischetti, E.M. Scheuring, W.X. Huang, Y. Hai, M. Sullivan, B. Sclavi)) Department of Physiology and Biophysics, Albert Einstein College of Medicine, Bronx, NY 10461

Time-resolved x-ray structural data has become feasible based on the high flux and brightness of synchrotron X-Ray beams. One of the most closely examined problems in this area of time-resolved structure determination has been the examination of intermediates in ligand binding to myoglobin. Recent crystallographic experiments using synchrotron radiation have identified the protein tertiary and heme structural changes that occur upon photolysis of the myoglobin-carbon monoxide complex (Schlichting et al. *Nature, 371,* p.808 (1994)). However, the precision of protein crystallographic data (~0.2 Å) is insufficient to provide precise metrical details of the iron-ligand bond lengths. Using time-resolved x-ray data acquisition techniques on microsecond to millisecond timescales along with simulations based on the *ab initio* Extended X-Ray Absorption Fine Structure code FEFF 6.01, we analyzed data taken on photolyzed solution samples of the myoglobin-carbon monoxide complex from 10-260 K. We provide precise metrical details for the Mb*CO state at 10 K and structural information based on x-ray edge data for microsecond and longer time relaxations above the glass transition. This research was supported by grants from NIH HL-45892 and RR-01633 and NSF BIR-9303830.

M-PM-G2

QUANTITATIVE DESCRIPTION OF OUT-OF-PLANE DISTORTION OF THE MACROCYCLE OF SYNTHETIC AND PROTEIN-BOUND PORPHYRINS.
((W. Jentzen,[1] X. Song,[1,2] J. A. Shelnutt[1,2])) [1]Fuel Science Department, Sandia National Laboratories, Albuquerque, NM 87185-0710. [2]Department of Chemistry, University of New Mexico, Albuquerque, NM 87131.

It has recently been recognized that the degree of nonplanarity of the porphyrin macrocycle may be important for controlling many basic biological processes such as electron transfer. For cytochromes *c*, for example, an energetically unfavorable, nonplanar distortion of the macrocycle is conserved, indicating that this out-of-plane distortion, which is primarily of the *ruffling* type, probably plays a significant role in its electron-transfer function. Besides this *ruffling* distortion, there are also some other basic non-planar distortions occuring in nature, namely *saddling, doming,* and *waving*. Interestingly, these basic distortions resemble the out-of-plane normal coordinates which have the lowest vibrational frequencies. This finding is physically reasonable because distortions along these out-of-plane normal coordinates require the least energy to overcome steric crowding of peripheral substituents and protein-porphyrin interactions. These interactions sometimes produce an overall out-of-plane distortion which cannot be described by purely one basic distortion. Consequently, a quantitative description of the out-of-plane distortions is necessary to gain more insight into which distortions are related to specific chemical and physical properties of the macrocycle. Thus, we have developed a method for decomposing the observed out-of-plane displacements of the macrocyclic atoms into contributions from out-of-plane normal distortions by using the lowest frequency out-of-plane normal coordinates as a basis set. This method is successfully applied to describe the out-of-plane distortions of X-ray crystal structures of synthetic and protein-bound porphyrins. (Supported by United States Department of Energy Contract DE-AC04-94DP85000 (JAS) and Associated Western Universities Postdoctoral (WJ) and Graduate Fellowship (XS).)

M-PM-G3

THE EXPOSED HEME PROPIONATES IN CYTOCHROME b_5 MODULATE ITS REDUCTION POTENTIAL. ((R. Seetharaman, and M. Rivera)) Department of Chemistry, Oklahoma State University, Stillwater, OK 74078. (Spon. by A. J. Mort)

Cyclic voltammetric experiments of outer mitochondrial membrane (OM) cytochrome b_5 and its dimethyl ester heme derivative were carried out at gold electrodes modified with β-mercaptopropionate. Reversible electron transfer was promoted by poly-*l*-lysine. Two molecules of poly-*l*-lysine bind per molecule of b_5. Binding of the first molecule of poly-*l*-lysine to OM b5 shifts the midpoint potential of the protein by approximately 50 mV, whereas binding of the second poly-*l*-lysine molecule alters the potential by only an additional 10 mV. Similar experiments carried out with the dimethyl ester derivative of OM b_5 show that the midpoint potential of this derivative changes only by 13 mV upon binding of two molecules of poly-*l*-lysine. This indicates that the first poly-*l*-lysine molecule to bind OM b_5 interacts with the heme propionates, therefore largely modulating themidpoint potential of the protein. Titration experiments in which the ^{13}C resonances of cytochrome b_5, whose heme has been enriched with ^{13}C at the heme propionates, were monitored as a function of poly-*l*-lysine, were used to corroborate the electrochemical observations. The unique role played by the exposed heme propionates of cytochrome b_5 in modulating the midpoint potential of cytochrome b_5 upon the formation of electrostatic complexes with redox partner proteins is discussed based on our electrochemical and NMR spectroscopic experiments.

M-PM-G4

NONPLANAR DISTORTIONS OF NICKEL(II) DIALKYLPORPHYRINS ALONG COMBINATIONS OF THE LOWEST-FREQUENCY OUT-OF-PLANE NORMAL COORDINATES ((X. Song,[1,2] W. Jentzen,[1] S. Jia,[1,2] L. A. Jaquinod,[3] D. J. Nurco,[3] G. J. Medforth,[3] K. M. Smith [3] and J. A. Shelnutt[1,2])) [1] Fuel Science Department, Sandia National Laboratories, Albuquerque, NM 87185-0710. [2] Department of Chemistry, University of New Mexico, Albuquerque, NM 87131. [3] Department of Chemistry, University of California, Davis, CA 95616.

Nonplanar distortions of the porphyrin macrocycle are commonly observed in crystallographic structures of tetrapyrrole-containing proteins. The types of symmetric distortions observed in crystallographic structures are the *ruf, sad, dom* and *wav* structures. These nonplanar distortioons closely match the eigenvectors of lowest-frequency out-of-plane normal modes (*ruf*~B_{1u} γ_{14}, *sad*~B_{2u} γ_{18}, *dom*~A_{2u} γ_9, *wav(x,y)*~E_g γ_{26}). Nonplanar distortions of the macrocycle occur easily along one of these soft normal coordinates for symmetrically substituted porphyrins. For asymmetrically substituted porphyrins such as the 5,15-dialkyl series, the nonplanar distortions occur along combinations of these lowest-frequency normal coordinates. More generally, any static nonplanar distortion of the macrocycle can be quantitatively described by a linear combination of the above eigenvectors. This is confirmed by decomposition of either the energy-minimized or crystallographic structures of all the conformers of nickel(II) 5,15-dialkyl-substituted porphyrins. The lowest-energy αα conformers show a *roof* structure which results from a combination of about 80% *ruf* and 20% *dom* structures. The higher-energy αβ conformers result from a combination of 50% *wav(x)* and 50% *wav(y)* structures. Quantum mechanical calculations were carried out on the energy-minimized conformers by INDO/s semiempirical method. The series of porphyrins were also studied by UV-visible and resonance Raman spectroscopies. The results show that the degree of nonplanarity increases as the steric bulk of the alkyl substituent increases.(Supported by United States Department of Energy Contract DE-AC04-94AL85000 and Associated Western Universities Fellowships (XS,WJ)

M-PM-G5

EXTENDED X-RAY ABSORPTION FINE STRUCTURE STUDIES OF THE ZINC DERIVATIVE OF CYTOCHROME *c*.
((H. Anni[1,2], J.M. Vanderkooi[1] and M.R. Chance[3]))
[1]University of Pennsylvania, Department of Biochemistry & Biophysics, Philadelphia, PA 19104; [2]Thomas Jefferson University, Department of Pathology, Anatomy & Cell Biology, Philadelphia, PA 19107; [3]Albert Einstein College of Medicine, Department of Physiology & Biophysics, Bronx, NY10461.

The Zn-edge extended x-ray absorption fine structure (EXAFS) studies of zinc(II)-substituted cytochrome *c* (Zn Cyt *c*) were undertaken in order to define the central metal environment and relative radial distances from ligands. The solution structure of Zn Cyt *c* suggested that Zn is in a unique hexa-coordinated state, N_5-Zn-S_1 (with five nitrogens and one sulfur ligand). Furthermore, the fluorescence line narrowing spectroscopy of Zn Cyt *c* has shown that Zn becomes penta-coordinated upon protein unfolding. The 100 K x-ray fluorescence spectra of Zn Cyt *c* were measured at BNL beamline X-9B using a sagitally focusing Si(111) monochromator and a Canberra 13-element solid-state detector. Sets of experimental data to theoretical curves (FEFF 6.01) using a novel refinement procedure will be reported.
This research was supported by NIH grants PO1GM48130 (JMV, HA) and RR01633 (MRC), and the University of Pennsylvania Research Foundation (HA).

M-PM-G6

RATE DISTRIBUTIONS IN CO GEMINATE REBINDING WITH CYTOCHROMES $P450_{CAM}$, $P450_{LM2}$ AND $P450_{SCC}$.
((C. Tetreau,[a] D. Lavalette,[a] C. Di Primo,[b] G. Hui Bon Hoa[b] & R. Lange[c]))
a) INSERM U350 , INSTITUT CURIE, 91405-Orsay France. b) INSERM U310, 75005-Paris, France c) INSERM U128, 34033-Montpellier France.

Since the prioneering work of Frauenfelder and his group 20 years ago, many laser flash photolysis studies of protein dynamics have been devoted to respiratory hemeproteins. Here, we have focused on another family of hemoproteins, cytochromes P450, which catalyze the oxidation of xenobiotics or endogenous compounds. The kinetics of CO geminate rebinding with three different enzymes, $P450_{cam}$, $P450_{LM2}$ and $P450_{SCC}$ have been studied at temperatures down to 77K. The influence exerted by substrate fixation upon the dynamics of CO rebinding was also examined using several substrates and analogues with different sizes and shapes.

Below 160K, non-exponential kinetics were observed and attributed to a distribution of frozen conformational substates reacting with slightly different rates. The underlying rate constant distributions were reconstructed from the Maximum Entropy Method. Depending on the nature of the enzyme, one or two bands were observed in the rate constant spectrum, indicating the contribution of one or two different subpopulations or processes. The comparison of the enthalpy distributions observed upon changing the protein or the substrate indicate that the ligand binding dynamics greatly depends on the structure of the heme pocket and of the substrate.

M-PM-G7

PROTEIN INTERACTIONS WITH VISCOUS COSOLVENTS : LIGAND ESCAPE RATE *versus* ROTATIONAL BROWNIAN DIFFUSION

((D. Lavalette, C. Tetreau, and M. Tourbez))
INSERM U350,Institut Curie, 91405-Orsay France.

The rate of ligand escape from respiratory proteins such as Myoglobin or Hemerythrin is characterized by a reciprocal power-law dependence on viscosity ($k \sim \eta^{-p}$, with $p < 1$), at variance with Kramers' theory which predicted that p=1. This has been attributed to partial screening of the solvent friction by the protein matrix.
Recently we have shown that the exponent p is a function of the cosolvent's molecular weight, suggesting that direct protein-solvent interactions rather than bulk viscosity are affecting local protein motions. We now show that the protein rotational correlation time (ϕ), though characterizing a large scale motion of the molecule as a whole, is also best described by $\phi \sim \eta^{q}$. Deviations of the Stokes-Einstein equation become apparent in the viscosity range 1-70 cP when the cosolvent's molecular weight exceeds about 5 kD. The molecular weight dependence of q is similar, though distinct from that of p.

M-PM-G8

THE ROLE OF SERUM ALBUMIN IN PORPHYRIN METABOLISM. A FLUORESCENCE STUDY. ((R. Galantai, E. Balog, F. Tolgyesi, J. Fidy)) Institute of Biophysics Semmelweis University of Med. Budapest (Spon. by J. Fidy)

The translocation of carboxylic porphyrins within cells has been studied by a model system in 10mM TRIS buffer at pH7.4. Unilamellar liposomes of L-α-phosphatidylcholine, dimyristoyl (DMPC) +5% L-α-phosphatidyl-DL-glycerol, dimyristoyl (DMPG) of 60nm size have been prepared by a sonication technique. The size of the liposome has been detected by dynamic light scattering, and was found to be stable under experimental conditions. Mesoporphyrin (MP) IX has been selected as carboxylic porphyrin because of its higher solubility in organic or aqueous solutions and precautions have been taken to avoid the formation of aggregates. The binding of the porphyrin to liposomes, to human serum albumin (HSA) and to HSA-liposome complexes have been compared on the basis of fluorescence spectroscopy, anisotropy decay and fluorescence lifetime measurements where the signal originated either from MP or from the single tryptophan of HSA. The time resolution of the data has been limited to decay times above 1ns, as a time domain technique with a ns flashlamp as excitation source has been used. The fluorescence parameters indicated that MP binds both to liposomes and to HSA with high affinity as shown by the association constants. When the binding of MP to liposome-HSA complexes have been studied, a preference for binding to HSA has been demonstrated. The transport of MP from the liposome to HSA through the aqueous phase could be excluded.

DNA/RNA/NUCLEIC ACIDS

M-Pos1

WHAT ARE THE MAIN FACTORS DETERMINING THE STRUCTURE OF THE IONIC ATMOSPHERE OF NUCLEIC ACIDS? ((Vitaly Buckin[1], Besik I. Kankiya[2], Victor Morozov and Luis A. Marky[1])) [1]Department of Chemistry, New York University, New York, NY 10003, USA; [2]Scientific Center of Radiobiology and Radiation Ecology, Georgian Academy of Sciences, Tbilisi 380003, Republic of Georgia.

We have used a combination of high precision ultrasonic velocity, density spectroscopy, and scanning microscopy techniques to investigate the changes in hydration upon substitution of sodium for magnesium ions in the ionic atmosphere of single-, double- and triple-stranded DNA and RNA molecules. This substitution results in a positive compressibility and volume effects that reflect a dehydration of the whole counterion-polymer system. For RNA and DNA double helices containing A•U or dA•dT base pairs, the absolute values of compressibility and volume effects correspond to outer-sphere complexes. This means that the dehydration of Mg^{2+} in the ionic atmosphere of these duplexes is small and that Mg^{2+} keeps its coordinated water. In the case of duplexes with dG•dC base pairs, poly(A) and poly(U) single strands, the inner-sphere type of Mg^{2+} binding is observed. Relative to a duplex, we did not find significant differences in the hydration parameters of the triple helix ionic atmosphere. Furthermore, the highest dehydration effect was observed for single stranded polymers, in spite of their lower linear charge density. These results suggest that the local structure of the nucleic acid ionic atmosphere is mainly determined by short range forces, including ion-water and nucleic acid-water interactions. The long range electrostatic interactions responsible for the condensation of counterions do not show significant influence on the local structure of the ionic atmosphere. Supported by Grant GM-42223 from the NIH.

M-Pos2

APPARENT CHARGE MEASUREMENTS OF DEOXYOLIGONUCLEOTIDES.
((John Wooll[1], Jonathan B. Chaires[2], Thomas M. Laue[1])) Department of Biochemistry and Molecular Biology, The University of New Hampshire, Durham, NH 03857. Department of Biochemistry, The University of Mississippi Medical Center, Jackson, MS 39216

The apparent charges (Q_{app}) of 20-residue-long single-, double - and triple-stranded DNA oligonucleotides were estimated from steady-state electrophoresis (SSE) and free-boundary electrophoretic mobilities. For both methods, measurements were made with varying field strengths, K^+ concentrations and oligonucleotide concentrations. Q_{app} from SSE decreases strongly with increasing oligonucleotide concentration, whereas Q_{app} from electrophoretic mobility is much less sensitive to the oligonucleotide concentration. With increasing field strength the magnitude of Q_{app} from SSE approaches the Q_{app} estimated from electrophoretic mobility.
This work was supported by grants NSF BIR 9314040 and NCI CA 35635

M-Pos3

SODIUM CONDENSATION AROUND DNA OLIGOMERS FROM MD SIMULATIONS. ((Nina Pastor and Harel Weinstein)) Dept. of Physiology and Biophysics, Mount Sinai School of Medicine, New York, NY 10029.

To be able to account for the effect of counterions in the formation of protein-DNA complexes, we have explored sequence dependent structural and dynamic properties of DNA on sodium condensation, and the influence of "end effects" on these properties. We have carried out molecular dynamics (MD) simulations with the CHARMM potential of 8 DNA dodecamers of different sequences and 2 decamers of the same sequence, one simulating a free decamer, the other simulating an infinite helix. The systems include explicit waters and enough sodium ions to ensure electroneutrality (no added salt condition, at an ionic strength of 0.36M), with periodic boundary conditions. The simulation times were >500 ps, without any constraints other than SHAKE applied to hydrogen containing bonds. We have studied the required equilibration times for the sodium population, and have followed the distribution of sodium atoms around the DNA, both globally and as a function of axial position along the DNA. From these simulations, we estimate the Manning radius to be very close to 5Å, in striking concordance with the estimated Debye length for the ionic strength in the simulated systems. The [Na+] within a 5Å shell around the free DNA is ~0.7M, in agreement with the Grand Canonical Monte Carlo estimates (Olmsted, M.C. *et al.* (1989) *P.N.A.S. USA* **86**, 7766-7770) for oligomers of such length. The contribution of "end effects" will be obtained from the comparison of the sodium distributions around the infinite helix and the free DNA.

Supported by a grant from the Association for International Cancer Research and by a Fulbright/CONACyT (Mexico) scholarship (to NP).

M-Pos4

Molecular Dynamics Simulation Of B-DNA With Explicit Counter-ions Using The CHARMM Force-field

(Aswin Dinakar, G. Ravishanker, D.L. Beveridge) Department Of Chemistry, Wesleyan University, Middletown, CT 06459.

Results from a nanosecond molecular dynamics study of the dodecamer CGCGAATTCGCG with explicit counter-ions and TIP3P waters will be presented. The focus of this study will be to show how the presence of counter-ions affect the fine structure of DNA. The use of protocols such as force-shifted function and ewald summation on the structure of DNA will be presented. The structure of ions and their correlated motions will be examined in this work. The current simulations will be compared with other simulations from our lab using other force-fields.